Second United Nations
International Conference
on the Peaceful Uses of
Atomic Energy

A/CONF.15/P/713
U.S.A.
June 1958

ORIGINAL: ENGLISH

# ADVANCES IN THE PHYSICAL METALLURGY OF URANIUM AND ITS ALLOYS

H. H. Chiswik, A. E. Dwight, L. T. Lloyd,
M. V. Nevitt and S. T. Zegler*

## INTRODUCTION

The physical metallurgy of uranium and its alloys was surveyed at the first International Conference on the Peaceful Uses of Atomic Energy in papers by Foote,(1) Saller and Rough,(2) and Pfeil.(3) The uranium-aluminum alloys were discussed in greater detail by Cabane, Englander and Lehmann,(4) and by Saller.(5) This paper presents a review of some advances in this field that have been made in the United States of America since the first Conference. The first part is devoted to unalloyed uranium; the second part deals with uranium alloys.

The major developments in the physical metallurgy of unalloyed uranium have been in measuring and evaluating the basic physical and mechanical properties of the pure material free from the contributing effects of the usual contaminants. The objectives have been to gain a better understanding of the structure and metallurgical behavior of the metal. The effort has been aided by studies on single crystals. In the alloy field the primary impetus has been to improve the two properties that are of greatest concern in the utilization of uranium as a fuel-element base material — the dimensional stability and corrosion resistance. Emphasis in this paper is centered, therefore, on high uranium-base systems which have shown promise in this direction. The properties of the alloys are discussed in relation to their constitution, heat treatability, transformation kinetics and micrographic features.

## UNALLOYED URANIUM

### Properties of Single Crystals

In metals possessing highly symmetrical crystal lattices the properties of the single crystals are not always predominant in determining the

*Argonne National Laboratory, Lemont, Illinois, U.S.A.

## DISCLAIMER

# DISCLAIMER

The enclosed document has not received any secondary reviews by the U.S. Department of Energy's Office of Scientific and Technical Information (OSTI) for public releasability Post 9/11. It is being made available with the understanding that any further distribution, beyond the requesting organization, is the responsibility of the receiving organization/individual. Any distribution outside the DOE community may require additional reviews by the originating site in compliance with Secretary Abraham's May 30, 2002, memorandum titled "Safeguarding Information Pertaining to Weapons of Mass Destruction and Other Sensitive Information."

properties of the polycrystalline aggregate; the properties of the latter are frequently controlled by variables which overshadow the basic properties of the individual crystals, e.g., grain boundaries, impurities, precipitates, and others. In orthorhombic alpha uranium, however, many of the physical and mechanical properties of the polycrystalline material are directly related to the anisotropy in the properties of the individual crystallites. In uranium, therefore, a knowledge of the properties of single crystals is especially helpful in that it provides a basis for correlating the properties of the polycrystalline material.

The crystal studies that are summarized below have been made on specimens prepared by the grain-coarsening technique described by Fisher.(6) To date this is the only method available for the preparation of relatively defect-free crystals. The specimens are small and not all types of measurements can be made on them. They frequently require extensive modifications in experimental techniques which subject some measurements to larger experimental errors than are usually encountered in similar experiments.

Electrical and Magnetic Properties: The electrical resistivities in the three principal crystal directions were determined by Berlincourt(7) at 273°K and 4.2°K:

| Crystal Direction | $\rho_{273°K}$ (micro ohm-cm) | $\rho_{4.2°K}/\rho_{273°K}$ |
|---|---|---|
| [100] | 39.4 ± 10% | $3.39 \times 10^{-2}$ |
| [010] | 25.5 ± 5% | $4.26 \times 10^{-2}$ |
| [001] | 26.2 ± 10% | $4.45 \times 10^{-2}$ |

Magnetoresistance measurements in transverse magnetic fields at liquid helium temperatures are shown in Fig. 1; the plots are linear at high fields and roughly parabolic at low fields. The magnetoresistance in a principal crystal direction as a function of the magnetic field orientation yielded sinusoidal curves with maxima and minima at the other two principal directions. Comparison of the data with similar measurements on other metals indicates that uranium is less magnetoresistive than Bi, Sb, Be, and As; roughly comparable with Th, Mg, Ga, Cd, Zn, Mo, Pb, and W; and more magnetoresistive than Ag, Au, Cu, Li, Pt, Al, In, K, and Na.

The superconductivity of a tri-crystal specimen has been studied by Hein, Henry, and Wolcott(8) down to 0.1°K. Although the superconductivity transition temperature is given as 0.68 ± 0.02°K, the transition occurred over the relatively broad temperature range of 0.45°K. Similar behavior was also noted in polycrystalline material of comparable purity.

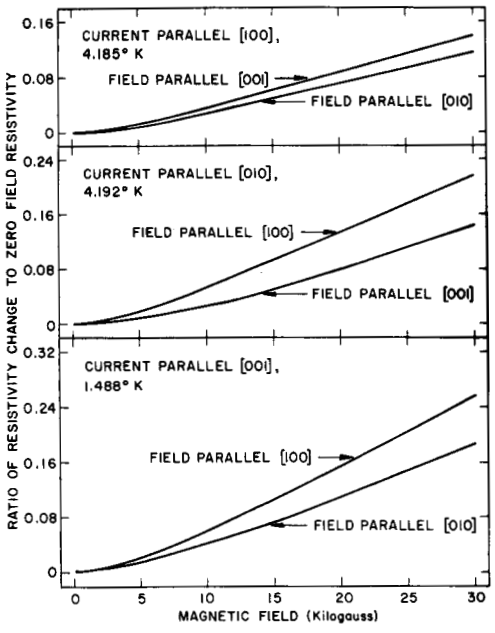


106-3758

Fig. 1

Effect of Magnetic Fields on Electrical Resistivity.[7]

Thermal Expansion: X-ray lattice parameter measurements have been extended by Bridge, Schwartz and Vaughan[9] to low temperatures. Linear and volume dilation equations fitted to the above data by least mean square methods[10] are:

$$L_{[100]t} = L_{[100]0°C}(1 + 22.50 \times 10^{-6}t + 11.97 \times 10^{-9}t^2 + 14.74 \times 10^{-12}t^3)$$

$$L_{[010]t} = L_{[010]0°C}(1 + 0.61 \times 10^{-6}t - 2.17 \times 10^{-9}t^2 - 18.41 \times 10^{-12}t^3)$$

$$L_{[001]t} = L_{[001]0°C}(1 + 19.37 \times 10^{-6}t + 5.71 \times 10^{-9}t^2 + 23.26 \times 10^{-12}t^3)$$

$$V_t = V_{0°C}(1 + 42.57 \times 10^{-6}t + 16.48 \times 10^{-9}t^2 + 18.80 \times 10^{-12}t^3)$$

where: V = volume, L = length and t = °C (-253° to 640°C)

An anomaly which is not understood was noted in the $a_0$ at low temperatures; the axis contracted normally down to 63°K but a measurement at 20°K suggested a reversal in the slope of the curve. Schuch and Lacquer[11] also noted an expansion in polycrystalline material upon cooling from 77°K to 20°K.

Dilation curves in the three principal directions are shown in Fig. 2. The single crystal data[12] agree with x-ray parameter values for the [100] direction, but are higher in the [001] direction and lower in the [010] direction. The discrepancies suggest that polycrystalline powders used in x-ray parameter determinations are subject to elastic restraints, induced by the anisotropy of thermal expansion, which affect the true thermal expansion characteristics of the lattice.

Klepfer and Chiotti[13] have measured the lattice parameters up to 1060°C; their data for the alpha phase agree with those of Bridge, Schwartz and Vaughan. The volume expansions as derived from their data are given in Fig. 3. The total volume change between 25°C and the melting point is 8.81%. The volume changes at the alpha⇌beta and beta⇌gamma transformations are 1.15% and 0.71% respectively.

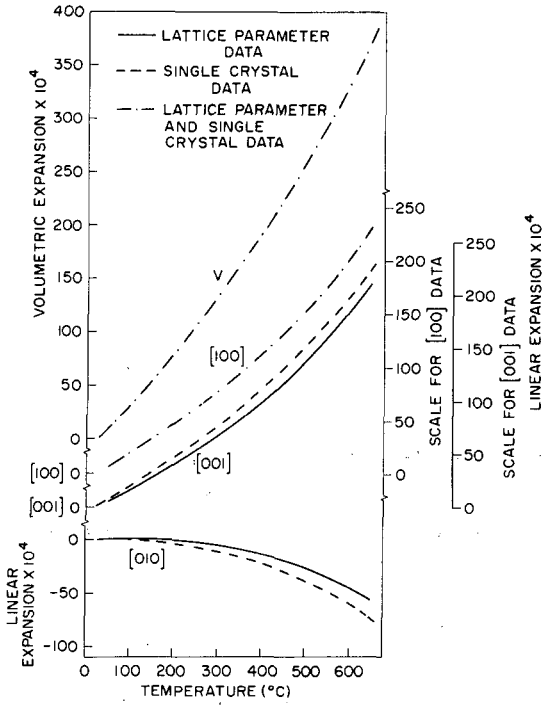


106-3755

Fig. 2. Thermal Expansion of Alpha Uranium.[9][12]

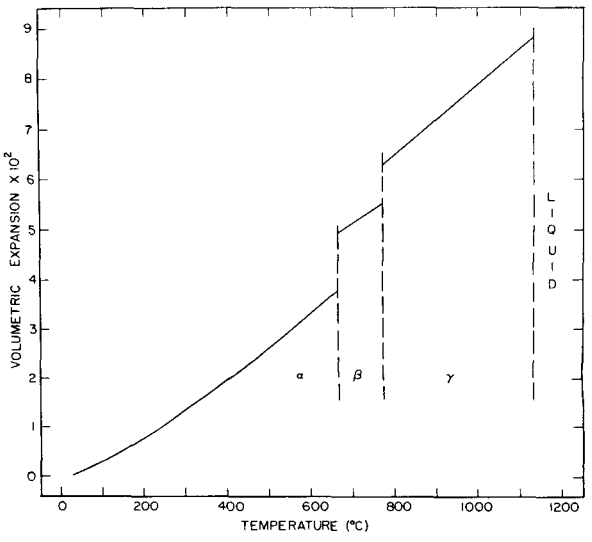


23,364

Fig. 3. Volumetric Expansion of Uranium.[13]

Elastic Constants: The nine fundamental moduli that are required to describe the elastic properties of the alpha uranium lattice have been determined by Fisher and McSkimin,[14] using an ultrasonic pulse technique especially adapted to the small crystals (Table I). The elastic constants derived from them are listed in Table II, and the variation of Young's Modulus with crystallographic direction is shown in Fig. 4.

Table I

FUNDAMENTAL ELASTIC MODULI OF ALPHA URANIUM SINGLE CRYSTALS AT 25°C.[14]

| Stiffness Moduli x $10^{-12}$ (dynes/cm$^2$) | Compliance Moduli x $10^{12}$ (cm$^2$/dyne) |
|---|---|
| $C_{11}$ = 2.1474 ± 0.14% | $S_{11}$ = 0.4907 |
| $C_{22}$ = 1.9857 ± 0.14% | $S_{22}$ = 0.6743 |
| $C_{33}$ = 2.6711 ± 0.14% | $S_{33}$ = 0.4798 |
| $C_{44}$ = 1.2444 ± 0.10% | $S_{44}$ = 0.8036 |
| $C_{55}$ = 0.7342 ± 0.10% | $S_{55}$ = 1.3620 |
| $C_{66}$ = 0.7433 ± 0.10% | $S_{66}$ = 1.3453 |
| $C_{12}$ = 0.4649 ± 0.58% | $S_{12}$ = -0.1194 |
| $C_{13}$ = 0.2177 ± 1.47% | $S_{13}$ = 0.0082 |
| $C_{23}$ = 1.0791 ± 0.71% | $S_{23}$ = -0.2627 |

Table II

ELASTIC CONSTANTS OF ALPHA URANIUM SINGLE CRYSTALS[14]

| Young's Moduli (E) | Linear Compressibilities ($\beta$) |
|---|---|
| $E_{[100]} = 2.038 \times 10^{12}$ dynes/cm$^2$ ($29.6 \times 10^6$ psi)<br>$E_{[010]} = 1.483 \times 10^{12}$ dynes/cm$^2$ ($21.5 \times 10^6$ psi)<br>$E_{[001]} = 2.084 \times 10^{12}$ dynes/cm$^2$ ($30.2 \times 10^6$ psi) | $\beta_{[100]} = 0.380 \times 10^{-12}$ cm$^2$/dyne<br>$\beta_{[010]} = 0.292 \times 10^{-12}$ cm$^2$/dyne<br>$\beta_{[001]} = 0.225 \times 10^{-12}$ cm$^2$/dyne |
| Poisson's Ratios ($\sigma$)[a] | Volume Compressibility:<br>$\beta_V = 0.897 \times 10^{-12}$cm$^2$/dyne |
| $\sigma_{12} = +0.243$<br>$\sigma_{21} = +0.177$<br>$\sigma_{13} = -0.017$<br>$\sigma_{31} = -0.017$<br>$\sigma_{23} = +0.390$<br>$\sigma_{32} = +0.548$ | Bulk Modulus:<br>$K = 1.115 \times 10^{12}$ dynes/cm$^2$ |

[a] $\sigma_{ij} = \dfrac{\text{compressional strain in j direction}}{\text{extensional strain in i direction}}$ for a tensile stress in the i direction; the subscripts 1, 2 and 3 refer to [100], [010], and [001] directions respectively.

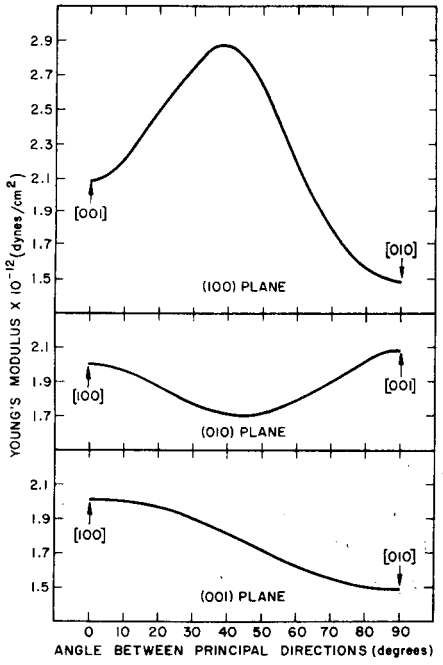


106-3757

Fig. 4

Variation of Young's Modulus with Crystallographic Direction.[14]

The minimum value of Young's Modulus occurs in the [010] direction, and the maximum is in a direction lying 38° from the [001] direction in the (100) plane. Using the method of Reuss as described by Hearmon,[15] the following values for randomly oriented polycrystalline material were derived by Rothman[16] from the single crystal data:

| | |
|---|---|
| Young's Modulus | $E = 28.3 \times 10^6$ psi |
| Shear Modulus | $G = 11.69 \times 10^6$ psi |
| Bulk Modulus | $K = 16.17 \times 10^6$ psi |
| Poisson's Ratio | $\sigma = 0.2087$ |

Plastic Deformation Mechanisms: The plastic deformation studies at ANL[17] have been extended to high temperatures; the results of compression at 600°C are summarized in Fig. 5.[12] Four operating slip systems have been identified; the following resolved shear stresses are required to initiate them:

| Slip System | Critical Resolved Shear Stress ($Kg/mm^2$) |
|---|---|
| (001) [100] | 0.024 |
| (010) [100] | 0.29 |
| {110} <110> | 0.39 |
| {021} <112> | 1.75 |

Using these values, the (001) projection quadrant in Fig. 5 is divided into approximate areas wherein the corresponding slip systems would be the first to operate. Most crystals deformed by more than one mechanism, including twinning on {130} and ~{172} when compressed in a direction close to the [010].

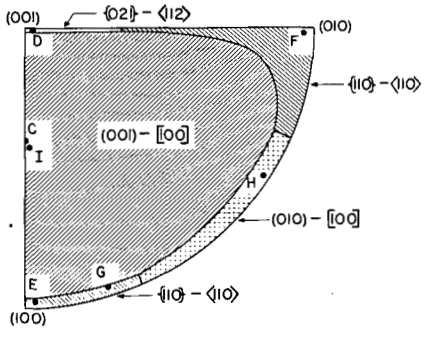


23279

Fig. 5

Slip Systems and Areas of their Operability in Uranium Single Crystals on Compression at 600°C.[12] Letters refer to directions that were investigated experimentally.

The low critical resolved shear stress of the (001) [100] slip system makes it the dominant deformation mechanism at 600°C. In room temperature compression this system was found to operate only as a minor contributing mechanism, in the form of cross-slip in conjunction with the major (010) [100] system. The (010) [100] and {110} <110> systems have comparable critical resolved shear stresses at 600°C. The {110} <110> system

was not observed in room temperature compression; its operability is apparently confined to higher temperatures. The high critical resolved shear stress of the {021} <112> system obviously makes it a relatively minor means of deformation at 600°C. It is of interest to note that slip in the latter system is not along the most densely packed direction - the [100] - but rather on the second most densely packed direction, the <112>.

## Polycrystalline Uranium

Recrystallization and Grain Refinement: Grain refinement of as-cast and beta treated wrought material has been studied as part of the general objective to alleviate the surface roughening problem, which has been shown to be primarily a function of grain size.[18] Powell, Klein and Krashes[19] have shown that the grain structure of cast uranium can be refined by heating to beta or gamma phase temperatures and water quenching. The grain size obtained on quenching from the beta phase was found to be independent of the time and temperature in the beta phase. Additional grain refinement was obtained by multiple quenching (Fig. 6). Repeated quenching was instrumental in breaking up the rim of columnar grains on the free surfaces. Quenching from gamma phase temperatures offered no advantages over beta quenching and generally gave less satisfactory results.

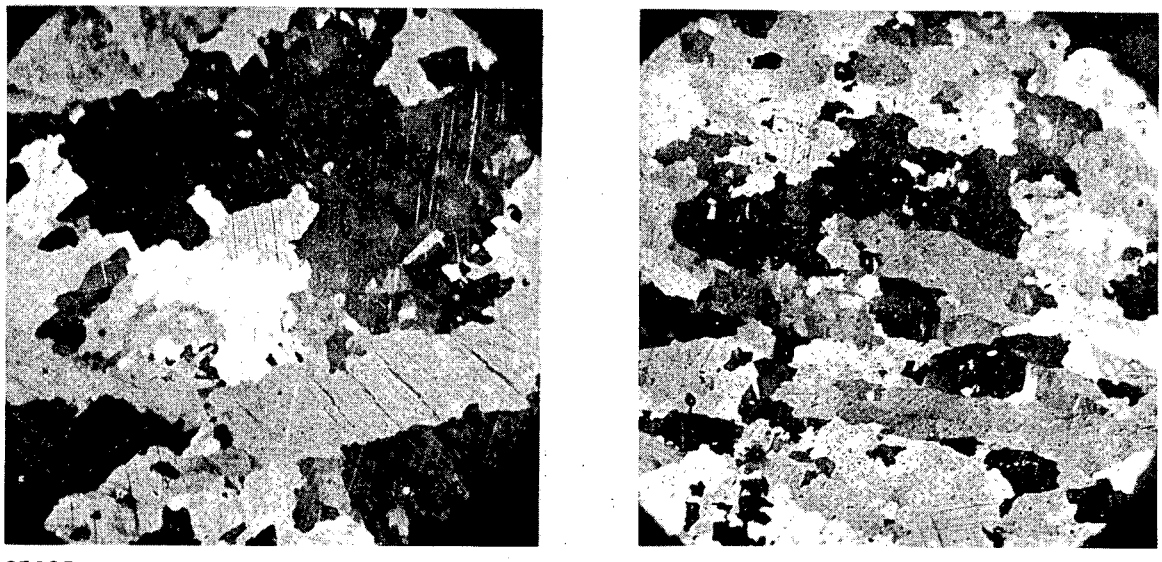


Fig. 6. Effect of Multiple Water Quenching from Beta Phase on Grain Structure of Uranium Castings.[19]

Recrystallization by alpha annealing subsequent to water quenching from the beta phase has been studied by Gardner and Riches.[20] The authors attribute the driving force for the recrystallization to the strains imparted to

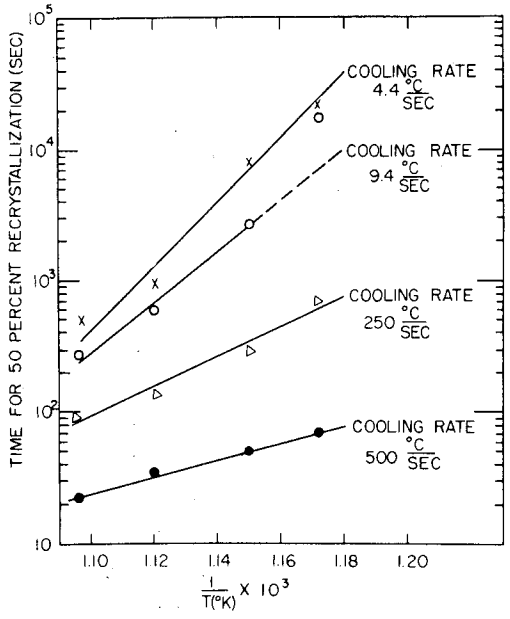


23284

Fig. 7. Time Required for 50% Recrystallization at Various Annealing Temperatures.(20)

the material during quenching, thereby making the kinetics of the process dependent upon the cooling rates. Plots of per cent recrystallization as a function of annealing time for various temperatures and various cooling rates yielded typical sigmoidal curves. The relationships of these variables are summarized in Fig. 7; the extent of grain refinement attained is shown in Table III.

Alpha ⇌ Beta Transformation: The heat treatment variables connected with this phase transformation have been studied in relation to the problem of attaining complete texture randomization on beta treatment. Orientation studies of individual large grains by x-ray back reflection Laue techniques in specimens slowly cooled from the beta phase under a temperature gradient have shown a concentration of (001) plane poles near the direction parallel to the temperature gradient.(12) The grains were generally elongated in the direction of the temperature gradient and the concentration of (001) plane poles in that direction increased as the temperature gradient was made steeper.

Table III

GRAIN REFINEMENT OF BETA QUENCHED WROUGHT URANIUM BY ANNEALING IN ALPHA PHASE(20)

| Cooling Rate During Quenching in 570 - 670°C Range (°C/second) | Average Grain Diameter | |
|---|---|---|
| | As Quenched | Alpha Recrystallized |
| 500 ± 100 | 0.20 | 0.08 |
| 250 ± 50 | 0.50 | 0.17 |
| 9.4 ± 2 | 0.55 | 0.40 |
| 4.4 ± 2 | 0.70 | 0.50 |

McDonell(21) has studied the effects of time, temperature and cooling rates on the loss of thermal expansion anisotropy of wrought uranium plate. The results are summarized in Figs. 8 and 9. Dilation curves in the longitudinal and transverse directions indicated a decreasing anisotropy as the time of heating at a given temperature was increased. The temperatures and times needed for complete loss of anisotropy were approximately:

| Temperature (°C) | Time (minutes) |
|---|---|
| 670 | > 60 |
| 675 | 20-30 |
| 680 | 8 |
| 685 | 3 |

At all temperatures grain coarsening proceeded at a more rapid rate than the loss of anisotropy. Specimens quenched into water were less anisotropic after a given time at temperature than corresponding air-cooled material.

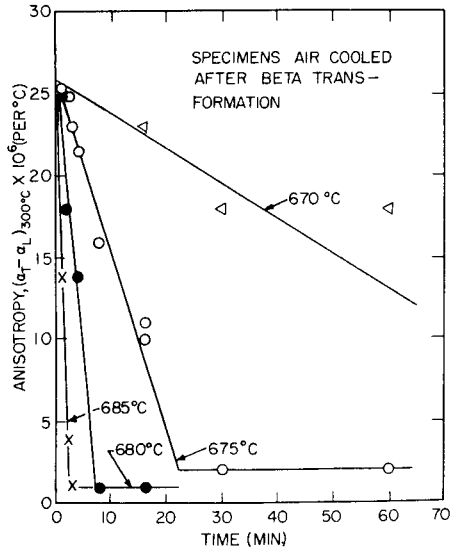


23298

Fig. 8. Loss of Thermal Expansion Anisotropy at Various Beta Transformation Temperatures.(21)

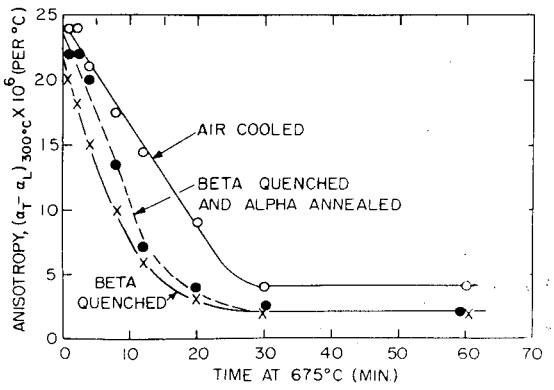


23297

Fig. 9. Influence of Cooling Rates on Loss of Thermal Expansion Anisotropy.(21)

To account for the differences between the rate of loss of anisotropy and the rate of grain coarsening, the author postulates that the transformation from the highly oriented alpha phase to the beta phase on heating is incomplete in short times at low beta phase temperatures, and that the residual alpha nuclei serve as centers for subsequent retransformation to an oriented large-grained alpha phase on cooling. The residual alpha nuclei thus preserve to some extent the preferred orientation of the wrought material. Water quenching increases the nucleation from the beta phase and, therefore, results in a more isotropic texture.

## URANIUM ALLOYS

The approach in the use of alloying to improve dimensional stability and corrosion resistance has been in two principal directions: (a) alloy

additions in relatively low concentrations designed to modify the kinetics of the beta or gamma phase decomposition so as to yield a structure combining random orientation and fine grain size; and (b) alloy additions in sufficient concentrations to stabilize partially or completely the cubic gamma phase, thereby circumventing the intrinsic instability of the orthorhombic alpha structure. The first group may be referred to as "alpha phase" alloys, the second group as "gamma phase" alloys. By restricting the alloy additions to low concentrations and to elements of favorable nuclear properties, the "alpha phase" alloys are best suited for the utilization of natural or slightly enriched uranium in thermal reactors. The "gamma phase" alloys are more suitable for fast reactors, since they require higher contents of alloying additions. The alloys discussed in this paper are mostly in the "alpha phase" group.*

## Effects of Low Alloy Additions on Dimensional Stability

Alpha Rolled Rods: The deformations that occur on cycling alpha rolled rods in the alpha phase temperature range stem from interactions between grains due to their anisotropic thermal expansions; the texture-dependent deformations take the form of gross elongations in the rolling direction.[18] Examples of the effects of molybdenum, silicon, aluminum, or zirconium additions are shown in Fig. 10. By comparison with 600°C rolled unalloyed uranium, it is apparent that such alloying additions do little to reduce the elongations of alpha rolled material. No special significance should be attached to the differences among the various alloy additions; they can probably be accounted for by variations in rolling temperature, cycling conditions, grain size, and possibly textural features, all of which have an effect on the magnitude of the elongations. The significant deduction to draw from these results is that alloying additions do not change the textural features in a manner that would decrease the elongations.

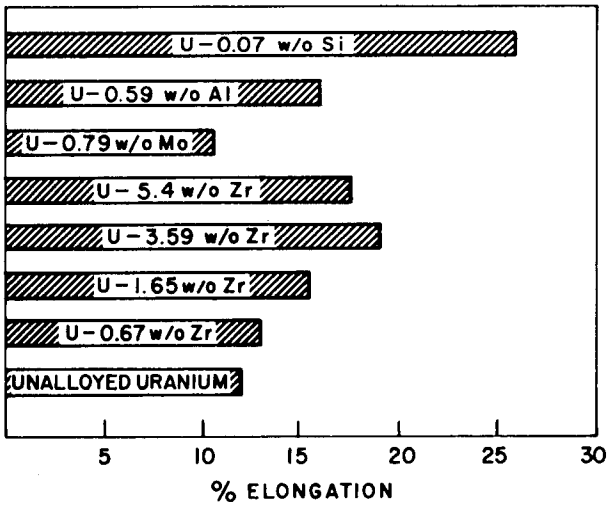


106-3738

Fig. 10. Elongations of Alpha Rolled Uranium-base Alloys after 700 Thermal Cycles between 100°C and 550°C.[22] Cycle: 5-7 minutes heating and 20-25 minutes cooling.

Heat Treated Alloys: Unalloyed uranium in the most suitably heated condition, that is after quenching from beta phase temperatures, retains evidences of preferred orientation, in that cycling causes slight preferential

*The "gamma phase" alloys are treated in detail in a separate paper at this Conference.

elongations and a roughening of the free surfaces. The extent of roughening has been shown to be primarily related to the grain size. Alloy additions have been found effective in alleviating this condition. To attain maximum benefits the alloys must be heat treated in a manner that will result in optimum grain refinement. The precise conditions vary with the alloying element addition, its concentration, the equilibrium phase relationships, and the manner in which it affects the subcritical transformation kinetics of the beta or gamma phase.

The effects of various alloy additions and heat treatments have been studied by Zegler and Chiswik.[22] Water quenching of alloys containing additions of 0.07 wt. % Si, 0.56 wt. % Al, 0.35 wt. % Ti, or 0.33 wt. % V from 710° - 725°C reduced the growth of alpha rolled rods to relatively low values; deformational changes after 700 cycles (100° - 550°C) were less than 2%, with some of the alloys exhibiting contractions rather than elongations. For the silicon, titanium, and vanadium alloys, this temperature range is in the beta phase; the aluminum alloy is in the $\beta + \delta$ ($UAl_2$) region. The alloys showed a lesser extent of surface wrinkling than unalloyed uranium similarly treated. Microstructurally, this heat treatment resulted in a relatively coarse alpha grain structure. The surface wrinkling corresponded with the observed grain structure; specimens having the coarsest grain structure exhibited the greatest degree of surface roughening.

Chromium additions in the equivalent concentration range as the above proved more effective. An alloy containing 0.39 wt. % chromium showed considerable improvement over unalloyed uranium. The optimum heat treatment was solution in the beta phase (700°C) and isothermal transformation at 475°C. Thermal cycling of this alloy under conditions that would yield a 6% elongation in the beta treated unalloyed uranium* resulted in an elongation of less than 0.5%. On the basis of the transformation kinetics reported by White[23] the above heat treatment corresponds to a decomposition of the beta phase in the temperature range of the upper "C" curve.

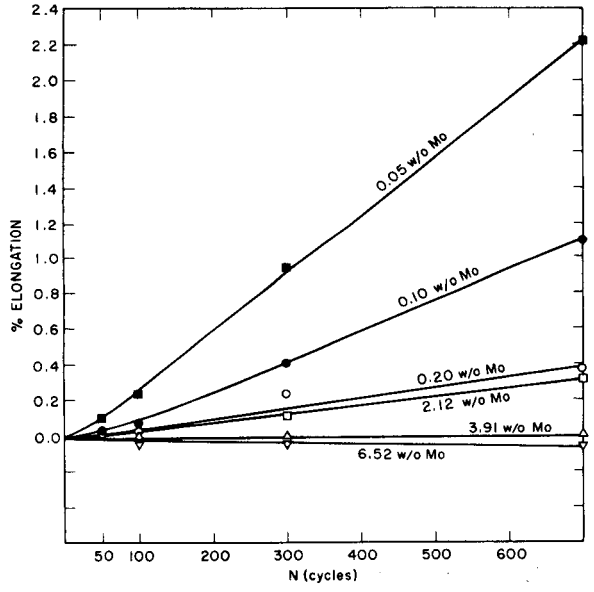


106-3737

Molybdenum additions up to about 2 wt. % did not completely eliminate the deformations (Fig. 11).

Fig. 11. Effects of Increasing Molybdenum Additions on Dimensional Stability. Alloys Quenched from Gamma Phase.[22]

*500 "slow heating - fast cooling" cycles 50° - 550°C.

Greater improvement was attained by water quenching from the gamma phase than by water quenching from the beta phase. The degree of improvement increased gradually with increasing molybdenum content. Specimens containing a minimum of 2 wt. % Mo remained essentially unchanged and their surfaces were smooth after 700 cycles (Fig. 12). Similarly good results were obtained on as-cast U-2 wt. % Mo alloys.

No systematic study was made on niobium additions. A uranium-0.6 wt. % Nb alloy casting showed no surface roughening and no elongations after 200 cycles. Niobium would therefore appear to be a particularly effective grain refinement agent.

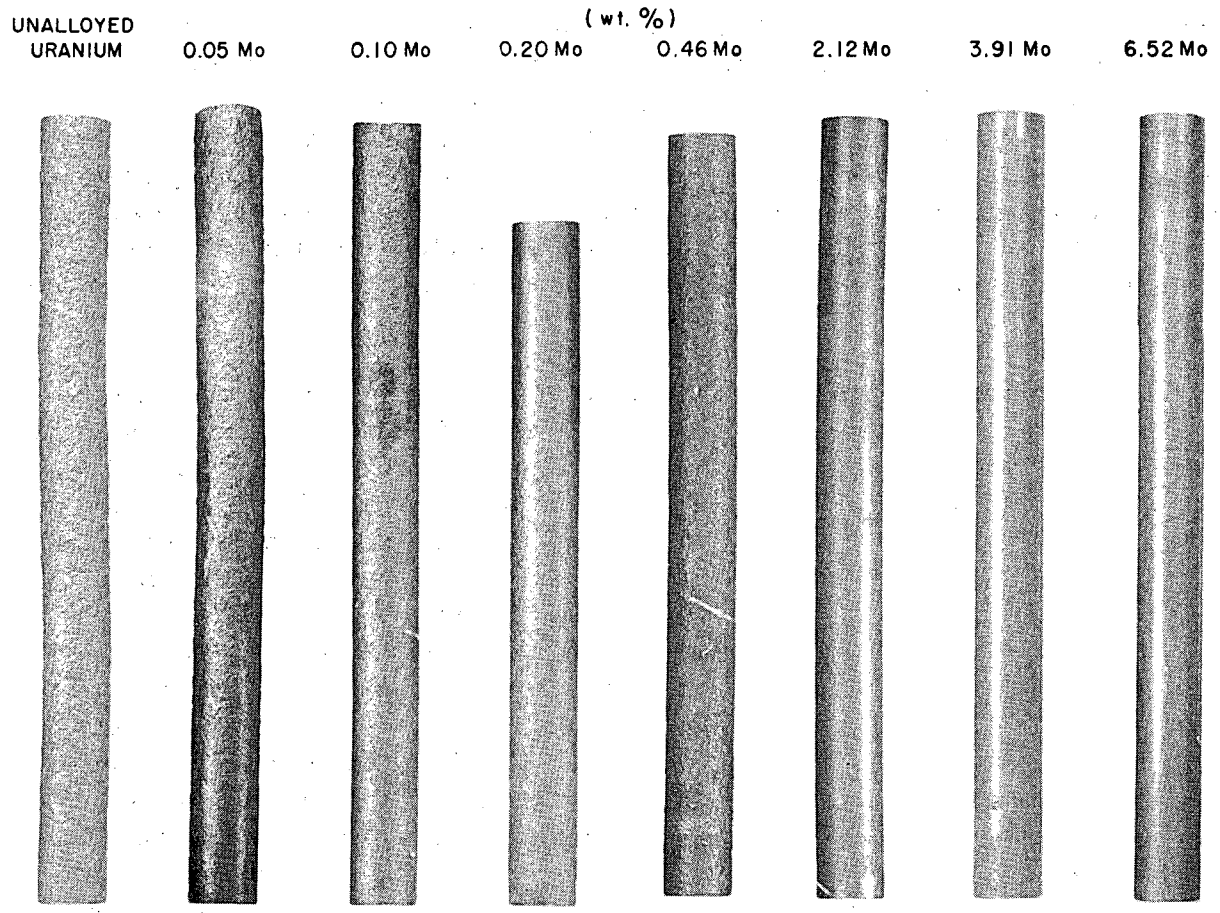


Fig. 12. Surfaces of Uranium - Molybdenum Alloys Water Quenched from 850°C and Annealed at 575°C.[22] 700 cycles; 100° - 550°C, 5 - 7 minutes heating and 20-25 minutes cooling.

Alloys containing up to 1.6 wt. % Zr had relatively large alpha grain structures following water quenching from beta or gamma phase temperatures, and attendant surface roughening on thermal cycling. As the zirconium content was increased to about 2 wt. %, the character of the water quenched microstructure changed to a fine grained acicular structure. A minimum zirconium content of about 2 wt. % was needed to attain smooth surfaces (Fig. 13).

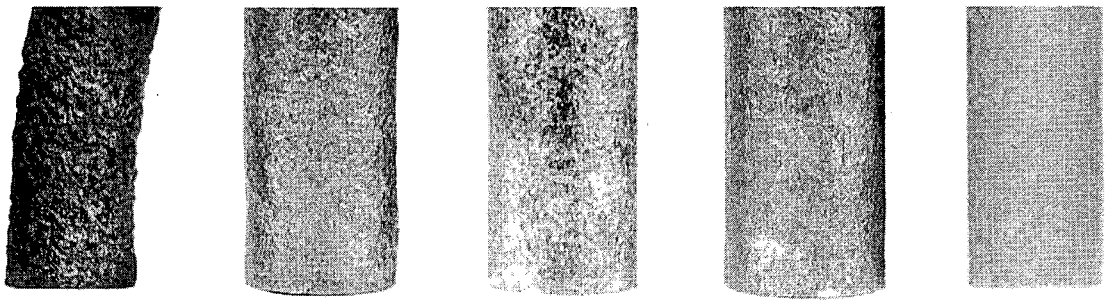


Fig. 13. Effect of Increasing Zr Concentrations on Surface Roughness of Heat Treated U-Zr Alloys,[12] 700 cycles; 100° - 550°C, 5 - 7 minutes heating and 20 - 25 minutes cooling. Alloys water quenched from the beta or gamma phase temperature.

The cooling rates from the gamma phase temperature affected the extent of deformation. Water quenching from 800°C was more effective than furnace cooling. The optimum heat treatment for stability in a U-2 wt. % Zr alloy was solution treating in the gamma phase followed by quenching to, and isothermally decomposing in, a temperature range of 500° - 575°C. Alloys treated in this manner showed negligible length changes after 1000 cycles and their surfaces remained smooth (Fig. 14). Alloys containing higher zirconium contents (5.4 wt. %) exhibited negligible deformations (< 0.2%) and no surface roughening even on furnace cooling.

Thermal Cycling to Beta Phase Temperatures: Repeated heating and cooling through the alpha $\rightleftharpoons$ beta phase transformation temperature causes a different type of deformation which has its origin in the widely different properties of the two phases, primarily density and mechanical strength. The deformations are directly related to the variables which affect the kinetics of the transformation, such as cooling rates, section size, and alloy content. The deformations may cause internal cavities and surface deteriorations far greater than the surface roughening obtained on cycling in the alpha phase temperature range. The effects of a number of low alloy additions on these deformations are shown in Fig. 15, based on studies by Hayward and Rowley.[24]

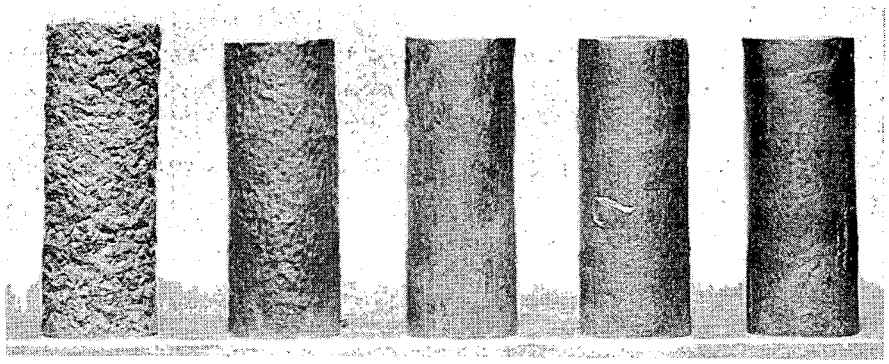


13,342

Fig. 14. Effect of Cooling Rate for 800°C on Surface Roughness of U-2 wt. % Alloys after 1000 Cycles between 50°C and 550°C.[12] Cycle: 15 minutes heating - 5 seconds cooling - 2 minutes holding time at limiting temperatures.

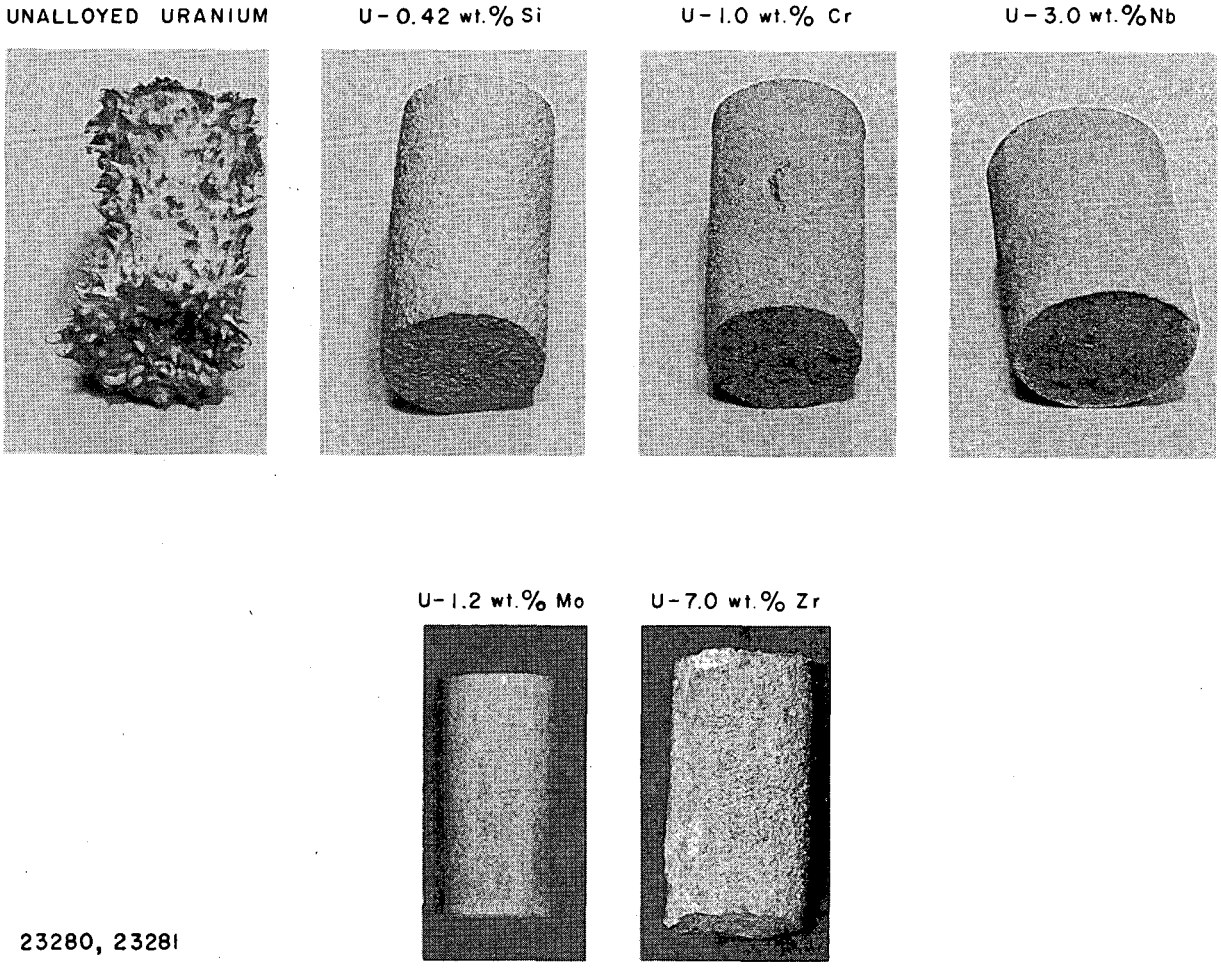


23280, 23281

Fig. 15. Effect of Alloying Additions on Alpha-Beta Cycling.[24] 500 Cycles 200° - 700°C.

The materials were cold pressed and sintered powder compacts. The most effective alloying element additions were Nb, Cr, Si, Mo, and Zr. The considerable improvement over unalloyed uranium is evident. None of the alloys developed internal voids.

## Uranium-Zirconium Alloys

The favorable nuclear properties of zirconium, its extensive solubility in gamma uranium and the attendant possibilities of property variation by heat treatment, coupled with its beneficial effects on the dimensional stability, all combine to make this metal a natural choice as an alloying additive to uranium for fuel element applications. The properties of the alloys with high zirconium contents are discussed in detail in another paper at this Conference; this section deals with the high uranium end of the system in the composition range of the minimal contents that were required to attain dimensional stability (2-3 wt. % Zr).

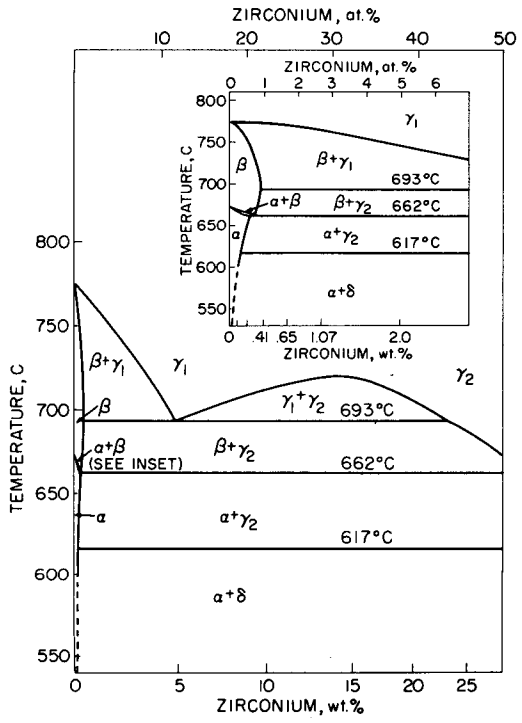


106-3741

Fig. 16. Uranium Rich End of the Uranium-Zirconium System.[12]

Phase Diagram: Certain conflicting features in the phase diagrams published by Saller and Rough[25] and Summers-Smith[26] have been reinvestigated by Zegler.[12] A revised version of the uranium-rich end is shown in Fig. 16. The monotectoid decomposition of $\gamma_1$ at 693°C and the eutectoid decomposition of $\beta$ at 662°C, as reported by Summers-Smith, have been confirmed. The $(\gamma_1 + \gamma_2)$ area boundaries have been relocated at 5.5 wt. % and 22.0 wt. % Zr at the monotectoid temperature. Oxygen and/or nitrogen were noted to have a pronounced effect on the temperature and composition limits of the miscibility gap; increasing concentrations enlarged the region with respect to both temperature and composition. The solubilities of Zr in alpha and beta uranium were found to be 0.2 wt. % at 662°C and 0.41 wt. % at 693°C respectively.

The delta phase region has been studied by Duffey and Bruch.[27] The phase is reported to form in uranium-rich alloys by a peritectoid reaction, $\alpha U + \gamma_2 \rightarrow \delta$ at 617°C and 39.0 wt. % Zr, and in zirconium-rich alloys by a eutectoid reaction, $\gamma_2 \rightarrow \delta + \alpha$ Zr at 606°C; the eutectoid composition is placed at 55 wt. % Zr. The structure of the delta phase has been studied independently by Boyko[28] and Mueller, Knott, and Heaton,[29] who report the phase

to be hexagonal with three atoms per unit cell located at 0, 0, 0; 1/3, 2/3, 1/2; and 2/3, 1/3, 1/2, with a c/a ratio of approximately 0.61. Certain compositions of this phase may also be considered to have a large cubic pseudo unit cell which may be derived from a twinning of the hexagonal cell, hence the observed cubic symmetry may be regarded as twin symmetry rather than crystal symmetry. The best agreement between calculated and observed intensities has been obtained with a partially ordered arrangement as suggested by Silcock,[30] in which zirconium is located at 0, 0, 0 and uranium and zirconium atoms are arranged in a random distribution on the other two sites. This results in an A-B layer structure of the C32 - $AlB_2$ type with alternate layers of zirconium atoms (A layer) arranged in a hexagonal basal plane array and a mixed uranium-zirconium atoms layer (B layer) in a graphite layer arrangement. Saller, Rough and Bauer[31] have determined the solubility of oxygen in the delta phase to be 500 ppm, and they suggest that in greater amounts oxygen and/or nitrogen result in the decomposition of the phase to alpha uranium and alpha zirconium.

Heat Treatment, Metallography, and Irradiation Stability: The microstructural features of castings and of wrought and heat treated 2 and 3 wt. % Zr alloys have been studied in relation to their effects on dimensional stability during irradiation.[12] The studies were prompted by observations that certain castings behaved better on irradiation than wrought alloys that had been heat treated to randomize the structure by water quenching from the gamma phase. The heat treatments included continuous cooling from the gamma phase at various rates, interrupted quenching, and quenching and tempering.

Referring to the phase diagram in Fig. 16, furnace cooling of alpha swaged rods from the gamma phase (800°C) produced a structure consisting of a two phase mixture suggestive of a eutectoid transformation (Fig. 17a). Water quenching yielded a finely acicular structure not unlike the structure described by Cabane[4] at the first Conference in the gamma quenched U-Al alloys (Fig. 17b). Intermediate cooling rates, such as air cooling and oil quenching, produced microstructures of an intermediate character, with increasingly more resistant etching characteristics as the quenching rate increased. Interrupted quenching and isothermal holding for 5-10 minutes at several temperatures between 400°C and 625°C yielded generally similar structures, with maximum hardness attained at about 400°C. Debye patterns of all these structures yielded diffuse $\alpha$ - uranium lines indicative of supersaturation. Castings generally responded to these heat treatments in much the same manner as alpha swaged rods.

Tempering the water quenched acicular structure in the $(\alpha + \delta)$ region at successively higher temperatures resulted in gradual spheroidization and and softening (Fig. 17c). The kinetics of the process are extremely slow, and several weeks at 575° - 600°C were insufficient to yield complete spheroidization and softening. Debye patterns after one month at 575°C showed

a. Furnace Cooled from 800°C

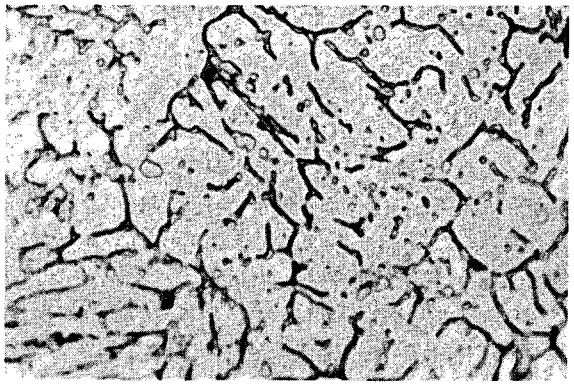

15,695 VHN = 253 2000 X

b. Water Quenched from 800°C

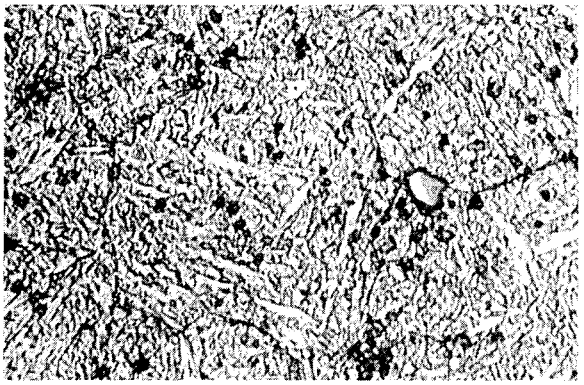

15,628 VHN = 403 1000 X

c. Quenched and tempered 2 weeks at 575°C

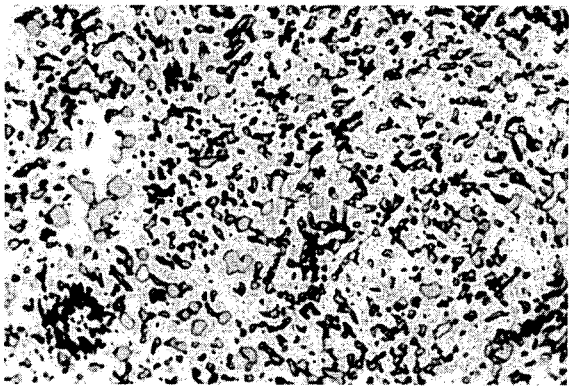

15,846 VHN = 293 2000 X

d. Quenched and tempered 2 weeks at 625°C

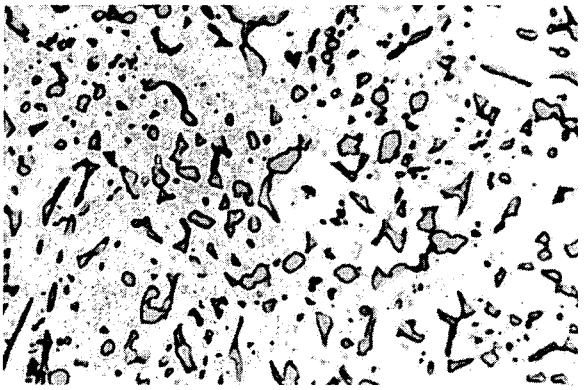

15,847 VHN = 259 1000 X

e. Quenched and tempered 1 week at 690°C

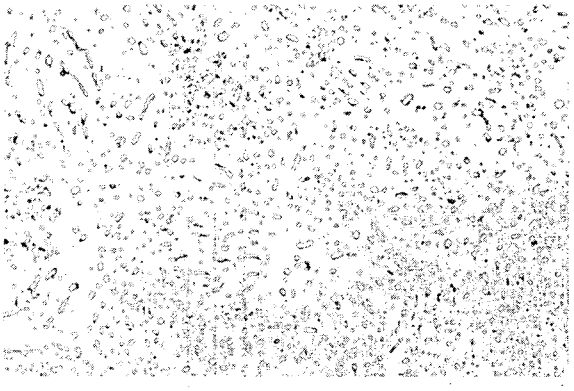

17,043 VHN = 254 500 X

f. Quenched and tempered 1 week at 725°C

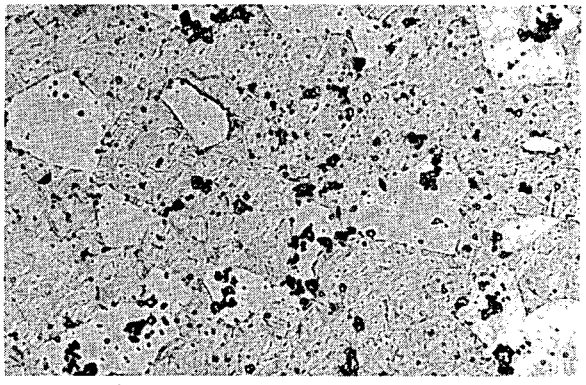

17,414 VHN = 495 (acicular) VHN = 360 (light) 500 X

FIG. 17. MICROSTRUCTURES OF U-2 WT. % ZIRCONIUM ALLOYS.[12]
(VHN - VICKERS HARDNESS NUMBERS)

a slight sharpening of the $\alpha$ lines, but gave no evidence of the spheroidal phase observed in the microstructure. Tempering in the range 300° - 400°C resulted in some precipitation hardening (Fig. 18).

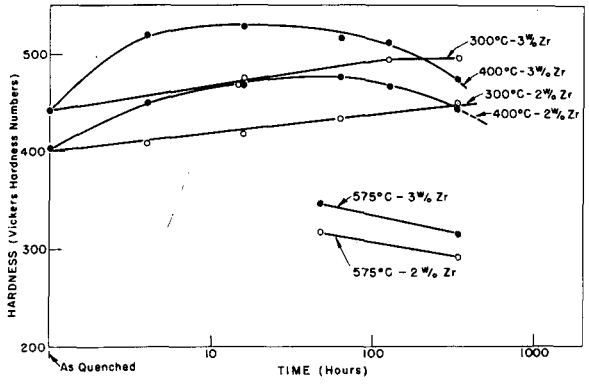


106-3734

Fig. 18. Hardness of Quenched and Tempered U-2 and 3 wt. % Zirconium Alloys.[12]

Tempering in the $(\alpha + \gamma_2)$ region and water quenching resulted in a duplex structure and further softening (Fig. 17d). Tempering in, and water quenching from, the $(\beta + \gamma_2)$ region yielded a finely spheroidal structure and the lowest hardness (Fig. 17e). On crossing the 693°C horizontal into the $(\beta + \gamma_1)$ region, the microstructure changed abruptly (Fig. 17f) and the hardness increased appreciably (Fig. 19). The interpretation of the microstructure is evident; the $\gamma_1$ has transformed to the acicular supersaturated alpha structure while the $\beta$ (light etching areas) transformed to normal alpha.

The relationship between heat treatment and irradiation stability is summarized in Table IV. Alpha swaged alloys elongated appreciably, in some cases even more so than similarly fabricated unalloyed uranium - a behavior quite analogous to the thermal cycling results. Heating in the $\gamma$ range and cooling to room temperature was sufficient to remove the major effects of the preferred orientation, but did not result in full stabilization; water quenching that yielded the acicular structure appears undesirable. Tempering this

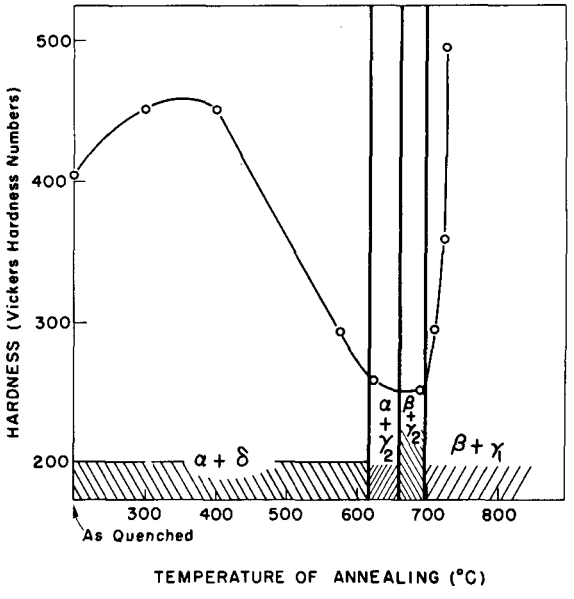


106-3735

Fig. 19. Hardness of Water Quenched and Tempered U-2 wt. % Zirconium Alloys.[12]

structure at successively higher temperatures to bring about spheroidization and softening showed a progressive improvement in stability, with the most stable alloys being those tempered in the $(\beta + \gamma_2)$ field. On tempering in, and quenching from, the $(\beta + \gamma_1)$ region where the resulting microstructure is again acicular, there is a deterioration in stability. The undesirability of the acicular structure is further demonstrated by the fact that castings which behaved rather well under irradiation showed a decrease in stability after water quenching. Other features worth nothing are: (a) stability was decreased by tempering in the temperature range 300° - 400°C where age hardening occurred; and (b) the 3 wt. % Zr alloy was less stable than the 2 wt. % Zr alloy.

Table IV

EFFECTS OF HEAT TREATMENT ON IRRADIATION STABILITY OF URANIUM - 2 AND 3 WT. % ZIRCONIUM ALLOYS[32]

| Heat Treatment | Growth Coefficient, $G_1$[a] | |
|---|---|---|
| | 2 wt. % Zr | 3 wt. % Zr |
| As Cast | 7.5, 8.2 | 5.7 |
| Cast and Water Quenched from $\gamma$ | 20, 28 | - |
| Alpha Swaged | 470 | 720 |
| Swaged and Water Quenched from $\gamma$ (800°C) | 61, 64 | 140 |
| Quenched and Tempered 1 - 2 weeks at: | | |
| (a) 400°C $(\alpha + \delta)$ | 87, 82 | - |
| (b) 575°C $(\alpha + \delta)$ | 50 | 99 |
| (c) 625°C $(\alpha + \gamma_2)$ | 43 | 77 |
| (d) 690°C $(\beta + \gamma_2)$ | 3.4 | - |
| (e) 725°C $(\beta + \gamma_1)$ | 27 | - |

[a] $G_i$ - elongations in microinches per inch per ppm burnup; total atom burnup $<0.1\%$; irradiation temperatures $<300$°C.

Uranium-Niobium Alloys

The high-uranium end of the U-Nb phase diagram has been investigated by Rogers et al.,[33] and by Dwight and Mueller[34] (Fig. 20). On the basis

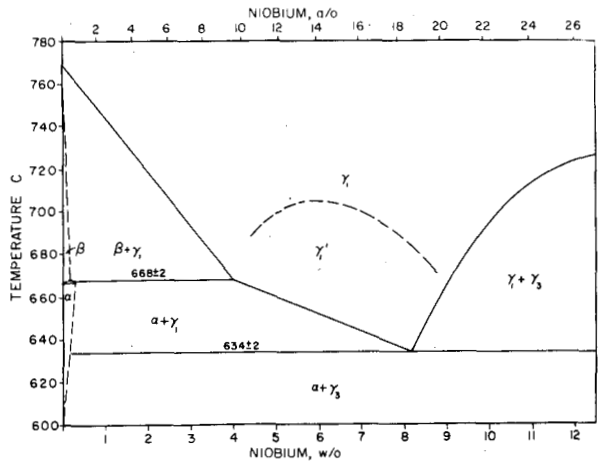


23218

Fig. 20. Uranium Rich End of U-Nb System.(34)

of the latter authors' work the monotectoid composition is located at 8.1 wt. % Nb and 634°C, which is at a higher Nb content and a lower temperature than previously reported.(25) A previously unreported from of $\gamma_1$ was observed between 4 and 9 wt. % Nb, designated $\gamma'_1$ in Fig. 20. Metallographically this phase is indistinguishable from the cubic $\gamma_1$; x-ray evidence, however, indicates what appears to be tetragonal symmetry, although its exact crystal structure is as yet undetermined. The phase is most readily obtained in the composition range 7.5 - 8.0 wt. % Nb in alloys annealed for long periods of time in the $\gamma'_1$ area. It was also obtained by tempering the metastable $\gamma_1$ phase in this composition range for short periods of time at temperatures below the eutectoid horizontal. The dotted line in Fig. 20 designating the temperatures of $\gamma_1 \rightarrow \gamma'_1$ transformation on slow cooling is based on thermal analysis data. The kinetics of its formation and the extra x-ray reflections suggest the likelihood of it being an ordered structure of the $\gamma_1$ phase.

The effectiveness of Nb in retarding the decomposition of the gamma phase is shown in the TTT curves of Fig. 21. The time-temperature relations for 1% transformation are shown for three compositions in the 60°C temperature intervals below their respective solvus temperatures. Niobium is not as effective a retarding element as molybdenum. The effect of Nb on the $M_S$ temperature is shown in Fig. 22 in comparison with Mo.

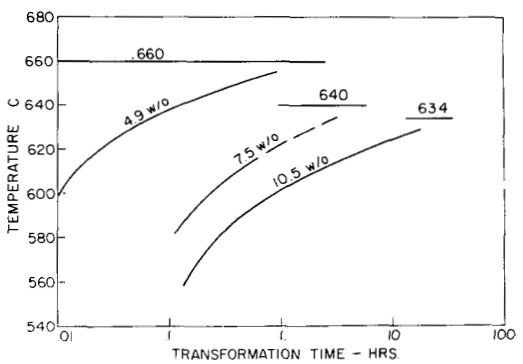


23240

Fig. 21. Time-Temperature-Transformation Curves for 1% Transformation in U-Nb Alloys.(12)

## Uranium-Zirconium-Niobium Alloys

Phase Diagram: The high uranium corner of the ternary system has been determined by Dwight and Mueller(34) in connection with the development of the U-5 wt. % Zr-1.5 wt. % Nb alloy fuel for the Experimental Boiling Water Reactor at ANL. The $(\gamma_1 + \gamma_3)$ area in the U-Nb binary system (from 8 to 55 wt. % Nb, above 634°C) is closed by the addition of less than 10 wt. % Zr. Increasing the zirconium content and lowering the temperature causes the

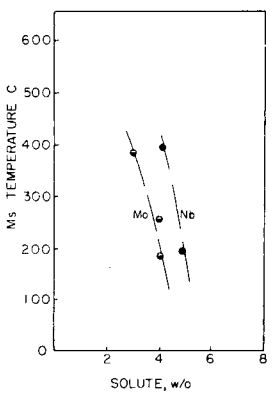


23250

Fig. 22. $M_S$ Transformation Temperatures of U-Nb and U-Mo Alloys.(12)

two terminal gamma phases to approach each other along an athermal valley, until they merge at a critical point. At zirconium contents above 10 wt. % a single gamma exists at high temperatures, which rejects alpha uranium at lower temperatures.

Similarly, the $(\gamma_1 + \gamma_2)$ area in the U-Zr binary system closes with the addition of approximately 1 wt. % Nb. Elimination of the two miscibility gaps leaves an extensive region of single gamma phase, as shown in Figs. 23 and 24. Addition of either niobium or zirconium stabilizes the gamma phase by depressing the temperature of the $\gamma \rightarrow \beta$ transformation. In alloys containing more than 4 wt. % Nb the $\beta$ phase is absent. The delta or $UZr_2$ phase extends into the ternary to no more than 10 wt. % Nb. Thus, over the major portion of the uranium-rich corner of the ternary system, the only equilibrium phases are the alpha and gamma uranium solid solutions. Figure 25 shows the vertical section through the uranium corner which includes the fuel alloy composition containing 5 wt. % Zr and 1.5 wt. % Nb. The sequence of transformations with decreasing temperature in this alloy is $\gamma_1 \rightarrow \beta + \gamma_1 \rightarrow \alpha + \beta + \gamma_1 \rightarrow \alpha + \gamma_1$.

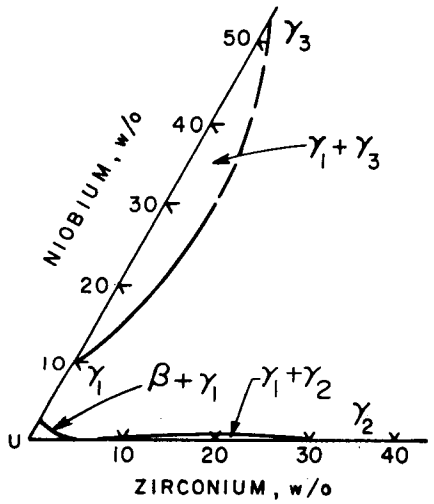


23231

Fig. 23. Isothermal Section of U-Nb-Zr System at 700°C.(34)

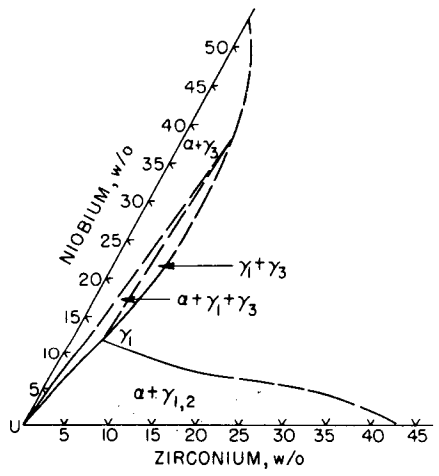


23233

Fig. 24. Isothermal Section of U-Nb-Zr System at 626°C.(34)

The line separating the $\gamma_1$ and $(\beta + \gamma_1)$ areas is concave toward the single phase $\gamma_1$ field (Fig. 23). The observed curvature of the line may be explained as due to the relief of lattice distortion in the gamma phase; niobium decreases the lattice parameter and zirconium increases it, with the

result that one solute relieves the lattice distortion introduced by the other. Because of this partial compensation, the gamma structure is enabled to exist at lower total niobium and zirconium contents than when either of these elements is present alone.

Transformation Kinetics: The subcritical transformation kinetics of several compositions at the 7 wt. % Nb level are shown in Fig. 26. The effect of increasing zirconium contents is such that the initial addition of 10 wt. % Zr greatly retards the transformation of the gamma phase, but a second addition to 20 wt. % Zr results in only a small further retardation. A possible explanation for the retarding action of zirconium is the observed tendency of zirconium to change the transformation product of the $\gamma_1 \rightarrow \alpha + \gamma_1$ reaction from a lamellar structure to a non-lamellar structure. Further increases in zirconium content, up to 30 wt. %, result in a marked retardation of transformation, which is probably explained by the close approach of this alloy to the composition at which gamma is stable down to room temperature.

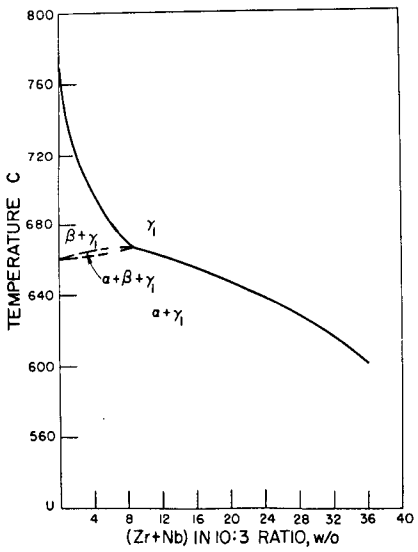


23232

Fig. 25. Vertical Section with Zr: Nb ratio of 5 to 1.5.[34]

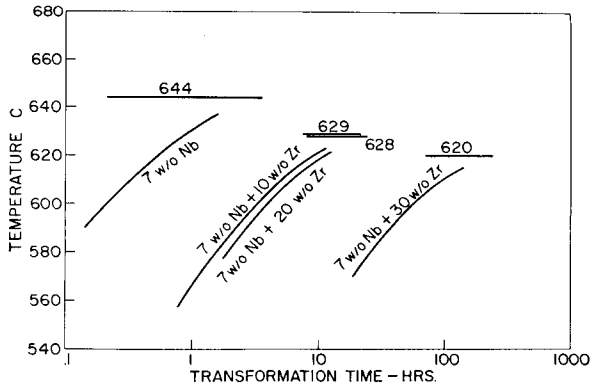


23241

Fig. 26. Effect of Zirconium Additions on Initiation of Subcritical Decomposition of U-Zr-Nb Alloys at 7 wt. % Nb Level.[12]

Corrosion Resistance and Irradiation Stability: The aqueous corrosion characteristics of the 5 wt. % Zr-1.5 wt. % Nb composition were discussed briefly by Foote[1] at the first Conference and have since been described in greater detail by Draley, Greenberg and Ruther.[35] This composition represents the minimal zirconium and niobium contents that were found necessary to attain satisfactory corrosion resistance in 300° - 350°C water; at the 5 wt. % Zr level, alloys with 1 wt. % niobium concentrations disintegrated after short periods of time at 300°C, and niobium concentrations beyond 1.5 wt. % did not result in further improvements. The average

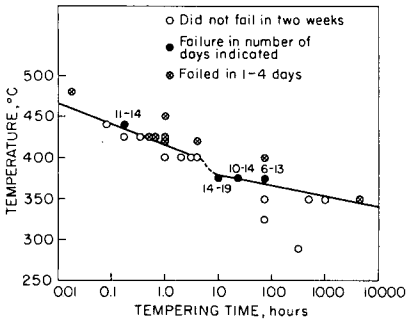


106-2481

Fig. 27. Effect of Tempering on Corrosion Life of Gamma Quenched U-5 wt. % Zr-1.5 wt. % Nb in 290°C Water.(35)

corrosion rate of the U-5 wt. % Zr-1.5 wt. % Nb alloy is given as 14-15 mg/cm$^2$/day. To obtain maximum corrosion resistance the alloy must be water quenched from the gamma phase to yield a martensitic plate-like structure. Tempering of this structure at low temperatures, although it produces no clearly visible changes in the microstructure, modifies the corrosion resistance and overaging destroys it. The effects of various tempering treatments are shown in Fig. 27; the area above the curve represents conditions which caused disintegration or failure by cracking in less than two weeks in degassed distilled water at 290°C; combinations of time and temperatures below the curve did not cause such failure.

The relationships between microstructure and irradiation stability were similar to those in the binary U-2 wt. % and 3 wt. % Zr alloys discussed in the previous section. The water quenched martensitic structures, as well as structures that were heat treated to high hardnesses, either by quenching and tempering at low temperatures or by isothermal subcritical transformation at low temperatures, had poor irradiation stability. As the tempering temperature increased, or as the isothermal transformation temperature was raised, the irradiation stability improved. Alloys that were fully transformed isothermally in the range 620° to 650°C exhibited the minimum irradiation growth (Table V). The latter treatment gave a microstructure of spheroidal alpha uranium particles in a gamma matrix. Precipitation of the alpha particles enriched the gamma phase in niobium and zirconium and permitted its retention at room temperature.

Table V

EFFECTS OF HEAT TREATMENT ON IRRADIATION STABILITY OF U-5 WT. % Zr-1.5 WT. % Nb ALLOY(12)

| Heat Treatment | $G_i$[a] |
|---|---|
| Water Quench from γ Phase | 290 |
| Oil Quench from γ Phase | 200 |
| Furnace Cooling | 17; 21 |
| Water Quenched and Tempered: | |
| (a) 72 hr. at 375°C | 210 |
| (b) 24 hr. at 650°C | 42 |
| Gamma Treated and Isothermally Transformed: | |
| (a) 10 min. at 475°C | 125 |
| (b) 30 min. at 650°C | 95 |
| (c) 24 hr. at 650°C | 5.4; 17 |

[a] $G_i$ - Elongations in microinches per in. per ppm burnup; total atom burnup $<0.1\%$; irradiation temperature $<300$°C.

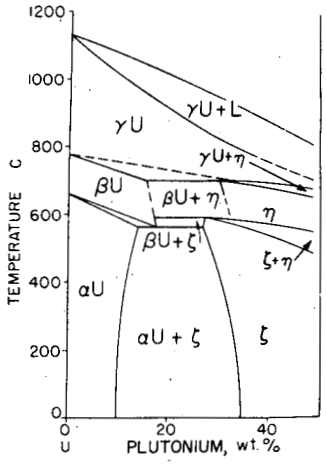


23245

Fig. 28. Uranium-Rich Portion of U-Pu Phase Diagram.(38)

## Uranium-Plutonium Alloys

The uses of plutonium in fuel elements for power reactors were discussed recently by Foote(36) and Kelman.(37) The undesirable properties of plutonium metal make it almost mandatory that it be used either as a dilute solute in solid solution or in the form of a physical dispersion in a suitable matrix. For applications in fast reactors uranium is an ideal matrix diluent. Interest in uranium-plutonium alloys is, therefore, largely confined to the high uranium compositions.

Figure 28 shows the uranium-rich portion of the uranium-plutonium phase diagram as determined by Schonfeld and co-workers.(38) The diagram is characterized by sharply decreasing liquidus and solidus temperatures and by a relatively restricted gamma field. Considering the limited solubilities of most other elements in $\alpha$ and $\beta$ uranium, the solubility of plutonium in these phases is rather extensive. The solubility of plutonium in beta is 18 wt. % at 600°C; alpha uranium can dissolve up to 15 wt. % plutonium at 560°C. Biver(12) has placed the room temperature solubility near 12 wt. % plutonium. Figure 29 shows the results of a study by Biver(12) of the variation of lattice parameters of alpha uranium with plutonium content. The very large change in $b_0$ with increasing plutonium content is notable, in contrast to the small changes of $a_0$ and $c_0$. Room temperature density measurements confirmed the density minimum at the alpha/alpha plus zeta phase boundary that is predicted by the parameter data and by the x-ray data of Coffinberry and Ellinger(39) for the zeta phase.

The properties of the uranium-rich alloys are generally poor. Unsatisfactory mechanical properties have been attributed to the presence of the zeta phase when the solubility limit in alpha is exceeded. Castings of alloys containing even small amounts of this phase are apt to contain microcracks and to disintegrate

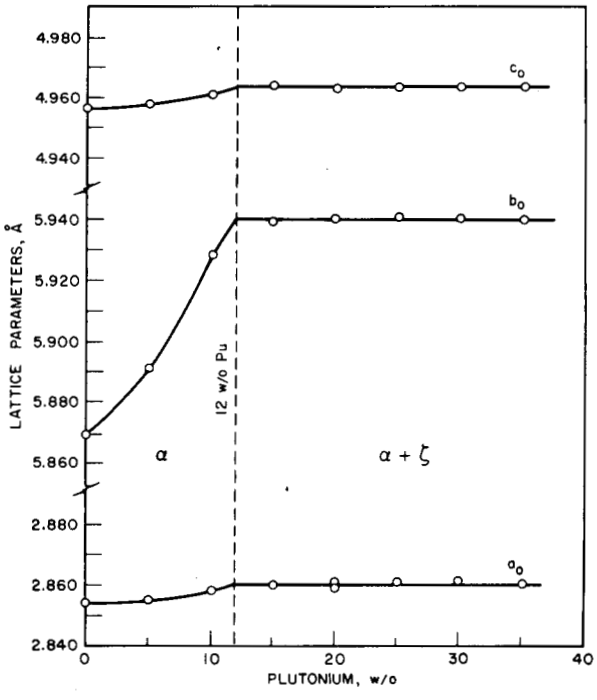


106-3764

Fig. 29. Lattice Parameters of Solid Solution of Plutonium in Alpha Uranium.(12)

on standing even in a helium atmosphere. Alloys containing 20 to 30 wt. % plutonium disintegrate more rapidly and are pyrophoric when exposed to air. The alloys are not fabricable even by hot rolling at 800°C; they have been extruded at 450° to 500°C. The hardness of castings increases from 59 $R_A$ to 69 $R_A$ with plutonium additions up to 20 wt. %. Their dilatometric behavior to 300°C is about the same as that of cast unalloyed uranium. Recent work by Biver[12] suggests, however, that the adverse properties are not inherent in the alloys but are due to either impurities or to the method of preparation; arc melted buttons containing up to 50 wt. % Pu were hot pressed and showed much less tendency to disintegrate on standing.

Uranium-Fissium Alloys

At the first Conference Feder[40] described a preliminary investigation of the role of oxidative slagging in reprocessing spent fuels of heterogeneous fast reactors. In the pyrometallurgical process, as it has been subsequently developed and modified,[41] decontamination with respect to volatile elements and rare-earths is quite good, but the fission elements Nb, Mo, Tc, Ru, Rh, and Pd remain in the fuel, and Zr is only partially removed. This complement of residual elements has been termed "fissium." A typical composition that might result after many reprocessing cycles using $U^{235}$ as the fissionable base material is given by Koch[42] as:

| | | | |
|---|---|---|---|
| Zirconium | - 0.10 wt. % | Ruthenium | - 2.63 wt. % |
| Niobium | - 0.01 wt. % | Rhodium | - 0.47 wt. % |
| Molybdenum | - 3.42 wt. % | Palladium | - 0.30 wt. % |
| Technetium | - 0.99 wt. % | Uranium | - 92.09 wt. % |

The major components in the fissium spectrum are molybdenum and ruthenium. The utilization of these complex uranium base alloys, with or without plutonium additions, as fuel materials in fast-breeder power reactors has been discussed by Foote,[36] Kelman,[37] and Koch.[42] This section deals with the physical metallurgy of the alloys in composition ranges bracketing the anticipated compositions that will result from the reprocessing cycle, including studies on the phase diagrams of uranium with some of the fissium elements.

Uranium-Ruthenium: The phase diagram up to $URu_3$ has been studied by Dwight[12] (Fig. 30). Gamma uranium dissolves a maximum of 5.5 wt. % Ru while the solubility in the beta and alpha phases is less than 1 wt. %. Both the gamma and beta phases can be retained by rapid quenching of small specimens. Six intermediate phases have been identified corresponding approximately to the stoichiometric ratios $U_2Ru$, URu, $U_3Ru_4$, $U_2Ru_3$, $U_3Ru_5$ and $URu_3$. Metallographic examination has placed the eutectic between gamma uranium and $U_2Ru$ at 899°C, while thermal analysis results by Park[43] indicate the values to be 890°C and 12 wt. % respectively. Transformations in

this system are very sluggish, which probably accounts for the lower eutectic temperature derived from thermal analysis. $U_2Ru$ and the beta uranium solid solution are the products of the eutectoidal decomposition of gamma uranium solid solution at 710°C and 2 wt. % Ru, and the beta in turn decomposes into alpha uranium and $U_2Ru$ at 633°C and 0.1 wt. %. $U_2Ru$, URu and $URu_3$ form peritectally at about 947°C, 1180°C and 1850°C respectively. The modes of formation of $U_3Ru_4$, $U_2Ru_3$, and $U_3Ru_5$ are not known; peritectic formations are probable, since the liquidus rises without open maxima to the melting point of ruthenium at 2500°C.(43) $U_3Ru_5$ decomposes eutectoidally at 870°C but can be retained by water quenching. Park reports the solid solubility of uranium in ruthenium is about 0.9 wt. % at 1500°C. None of the crystal structures of the intermediate phases have been determined other than that of $URu_3$, which has been identified as the $Cu_3Au$-type by Heal and Williams.(44)

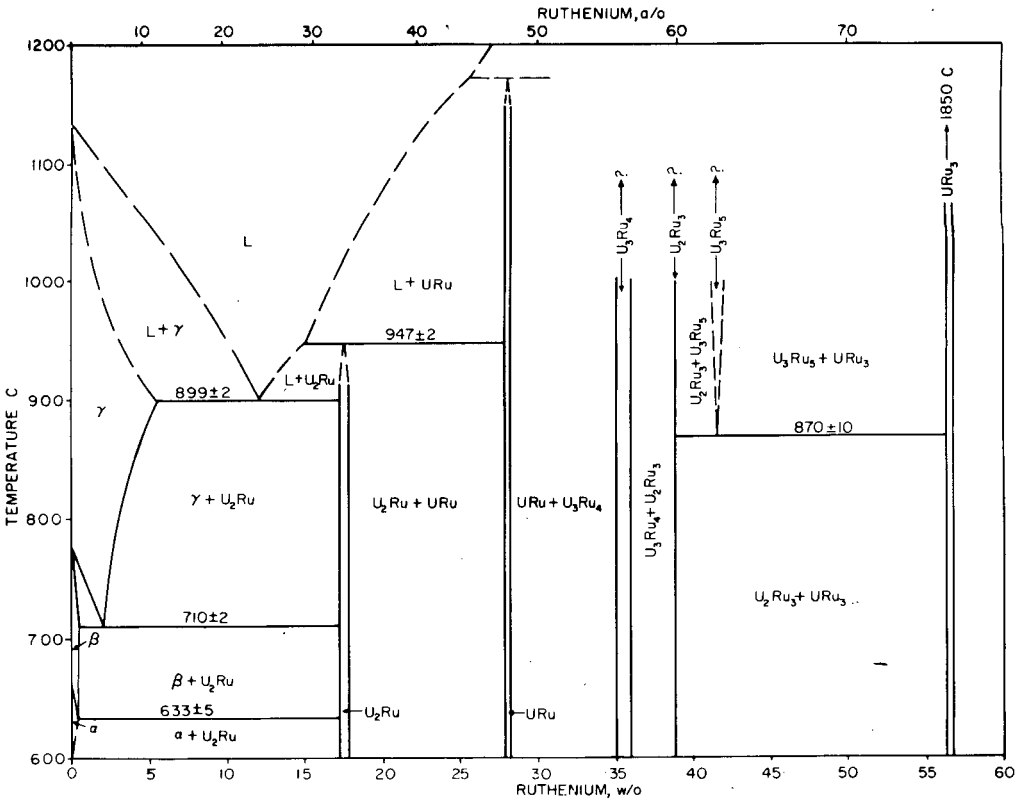


Fig. 30. Uranium -Ruthenium Phase Diagram.(12)

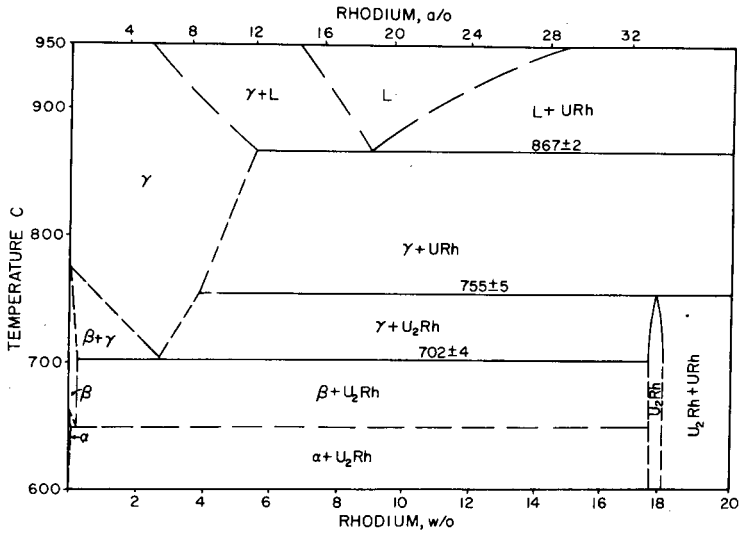


23224

Fig. 31. Uranium-Rhodium Phase Diagram.(12)

Uranium-Rhodium: The diagram up to URh resembles the U-Ru diagram except that the phase $U_2Rh$ forms peritectoidally rather than peritectically(12) (Fig. 31). As determined metallographically, the gamma phase is stable down to 702°C. Thermal analysis data(43) yielded 684°C for this transformation and 629°C for the eutectoidal decomposition of beta. The transformations are sluggish and susceptible to undercooling. The maximum solubilities of Rh in the gamma, beta and alpha phases are close to those of Ru in uranium. $U_2Rh$ forms peritectoidally at 755°C. The structures of $U_2Rh$ and URh are not known; $URh_3$ is isomorphous with $URu_3$, having the $Cu_3Au$-type structure. Thermal analysis places the liquidus in the vicinity of URh at about 1200°C. The liquidus continues to rise with higher rhodium content, suggesting that URh forms peritectically. The liquidus rises to a maximum at about 2160°C and 63 wt. % Rh, then falls to 1500°C at 78 wt. %.

Uranium-Ruthenium-Molybdenum: The uranium-rich corner of the system has been investigated from 600°C to 900°C.(12) Isothermal sections at 660°C and 900°C are shown in Figs. 32 and 33. At the upper end of this

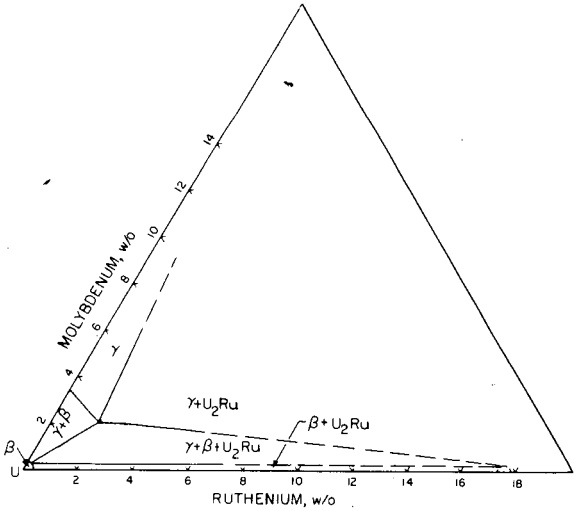


23223

Fig. 32. Isothermal Section of U-Ru-Mo System at 660°C.(12)

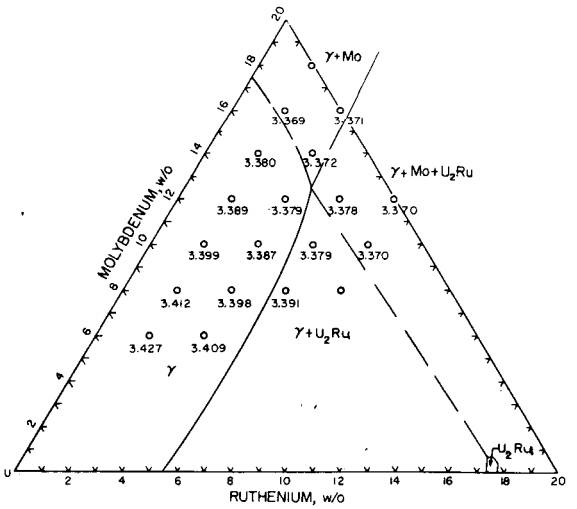


23222

Fig. 33. Isothermal Section of U-Ru-Mo System at 900°C and Gamma Phase Lattice Parameters, Å.(12)

temperature range an extensive gamma solid solution field exists, and the gamma phase can be retained to room temperature by quenching. Molybdenum and ruthenium are substantially interchangeable in their contracting effect on the gamma lattice parameter even though their atomic radii differ appreciably. At lower temperatures the gamma region retreats toward the uranium-molybdenum binary side. Molybdenum and ruthenium replace each other in solution in the beta phase and the ternary beta phase is stable down to a lower temperature than are the binary beta phases. At still lower temperatures a large three phase field exists due to the very restricted solubility of molybdenum and ruthenium in alpha uranium, and of molybdenum in the $U_2Ru$ phase. Figure 34 shows a portion of a vertical section in which the Mo:Ru is 2.5:2 by weight. This ratio approximates the proportions of the two elements in the uranium-fissium alloys. Reference to the vertical section is helpful in the interpretation of the transformations in uranium-fissium alloys as discussed in the section below.

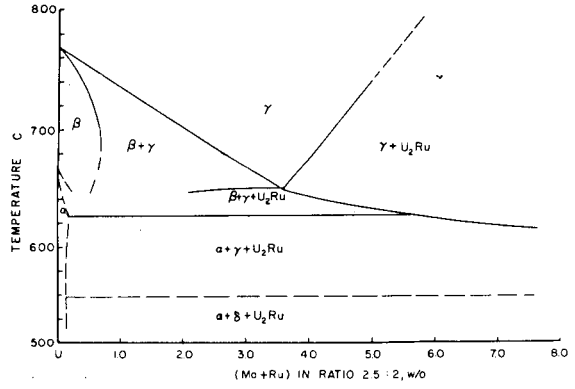


23219

Fig. 34

Vertical Section with Mo: Ru Ratio of 2.5:2.[12]

Transformation Kinetics: Structures and transformation temperatures of uranium-fissium alloys have been studied in specimens synthesized from stable isotopes with substitutions of molybdenum and ruthenium for technetium (Table VI).[12] One of the alloys contained higher zirconium (2.5 wt. %) in order to simulate a composition that might result from a variation of the pyrometallurgical refining process.

Table VI

COMPOSITIONS OF URANIUM-FISSIUM ALLOYS[12]

| Alloy | Fissium Element, wt. % | | | | | |
|---|---|---|---|---|---|---|
| | Mo | Ru | Rh | Pd | Zr | Nb |
| U-3 wt. % Fs | 1.4 | 1 | 0.2 | 0.1 | 0.03 | 0.006 |
| U-5 wt. % Fs | 2.4 | 2 | 0.3 | 0.2 | 0.05 | 0.01 |
| U-8 wt. % Fs | 3.8 | 3 | 0.4 | 0.3 | 0.07 | 0.02 |
| U-10 wt. % Fs | 4.8 | 4 | 0.6 | 0.4 | 0.1 | 0.02 |
| U-5 wt. % Fs-2.5 wt. % Zr | 2.4 | 2 | 0.3 | 0.2 | 2.3 | 0.01 |

Despite the complexity of the alloy compositions, it has been found that a straightforward interpretation of the transformations and resulting structures can be made in terms of the dominant U-Ru-Mo ternary system and the transformation kinetics of the alloyed uranium gamma phase. All the alloys are characterized by sluggish transformation kinetics. In the U-3 wt. % Fs alloy the gamma phase remains stable down to approximately 713°C, where a rejection of beta begins. At about 627°C beta decomposes eutectoidally to alpha plus gamma plus a compound which, from microscopic evidence, appears to be based on $U_2Ru$. A lower temperature transformation involving the formation of the delta phase of the U-Mo system has not been observed. Moderate cooling rates result in an alpha plus gamma structure, and even drastic quenching does not retain an all-gamma structure. Retained metastable gamma decomposes upon reheating to 300°C.

In the U-5 wt. % Fs alloy the gamma phase begins to precipitate the compound mentioned above at 749°C during slow cooling (0.75°C/min). The eutectoidal beta decomposition is apparently missed, and alpha is rejected at 608°C. A substantially all-gamma structure is easily retained upon quenching. Weak x-ray diffraction lines of gamma persist after very slow cooling from 850°C and in quenched samples tempered 24 hr. at 500°C. This indicates either that the last of the retained gamma decomposes very slowly, or that it is one of the stable phases at low temperatures.

The behavior of the U-8 wt. % Fs alloy and the U-10 wt. % Fs alloy is characterized by increasing sluggishness of the transformations. A structure that is substantially all-gamma is retained at practically all cooling rates.

The behavior of the U-5 wt. % fissium-2.5 wt. % Zr alloy is markedly different from the U-5 wt. % fissium alloy because of the "gettering" action of zirconium for ruthenium. The ZrRu phase is readily distinguishable in the diffraction pattern and microstructure of this alloy. The effect of the "gettering" action is to produce a gamma lower in alloy content and more similar in transformation characteristics to the U-3 wt. % fissium alloy.

Physical Properties: Saller et al[45] report liquidus and solidus temperatures of 1081°C and 1002°C respectively for a U-5 wt. % fissium alloy.

Room temperature density values for as-cast specimens are shown in Fig. 35. The density is linear with fissium concentration for alloys having a retained gamma structure but relatively higher for the U-3 wt. % fissium alloy whose structure is a mixture of gamma and the higher-density alpha phase. The density of a U-20 wt. % Pu-10 wt. % fissium alloy is reported by Dunworth[12] to be 16.75 gm/cc.

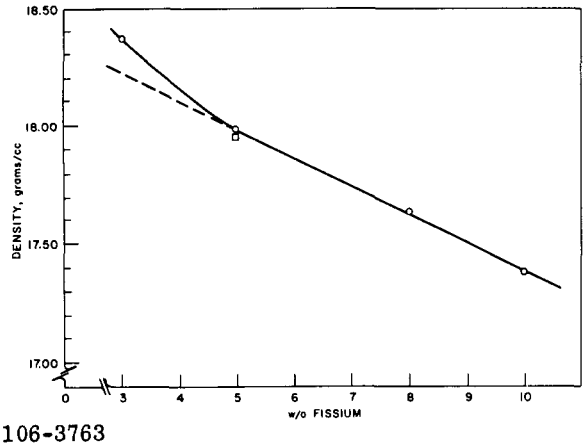


106-3763

Fig. 35

Room Temperature Densities of Uranium-Fissium Alloys.[12]

Figure 36 shows the linear thermal expansion curves of the U-5, 8 and 10 wt. % fissium alloys. The specimens were prepared from as-cast material and cycled twice between room temperature and the elevated temperature. Heating and cooling rates were between 1°C/min. and 2°C/min. The contractions between about 350°C and 450°C during the first heating correspond to the decomposition of the retained gamma phase. In the U-5 wt. % fissium alloy the cooling rate during the first cycle was not fast enough to retain metastable gamma, hence the contraction is absent during the second heating. For the higher fissium concentrations some gamma is retained, and it decomposes again upon reheating. The inflections are consistent with the phase transformations deduced from thermal analysis and metallography.

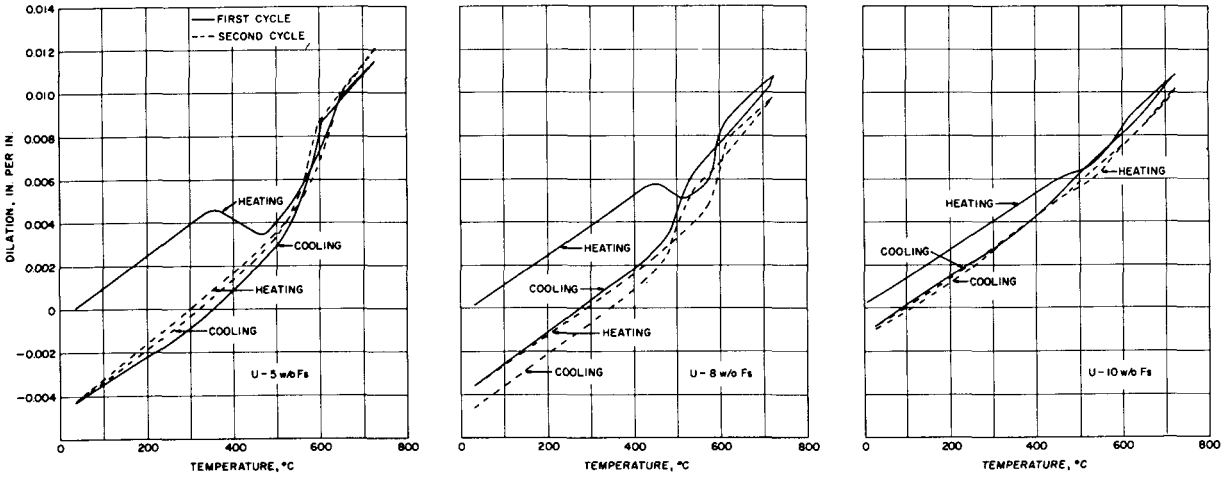


106-3761

Fig. 36. Linear Thermal Expansions of Uranium-Fissium Alloys.[12]

In Fig. 37 is shown the thermal conductivity of a U-5 wt. % fissium alloy[45] and of a U-20 wt. % Pu-10 wt. % fissium alloy obtained by Dunworth.[12] The conductivity of the U-5 wt. % fissium alloy increases more rapidly with temperature than that of uranium, so that the conductivities are equal at approximately 800°C.

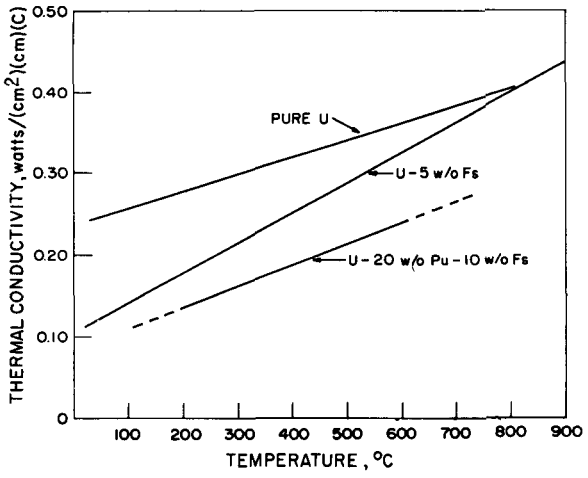


106-3762

Fig. 37

Thermal Conductivities of Fissium Alloys.(45)(12)

As-cast or heat-treated wrought specimens of a U-5 wt. % fissium alloy that were thermally cycled 250 times from 66° to 620°C showed negligible growth and no surface roughening.(46) Likewise, no significant dimensional changes resulted from the experiments of Sowa and co-workers,(47) wherein full size EBR-II fuel elements containing injection cast fuel pins of the alloy were cycled 200 times to 550°C.

## REFERENCES


1. Foote, F. G., Physical Metallurgy of Uranium, Proceedings of the International Conference on the Peaceful Uses of Atomic Energy, Vol. 9, paper P/555, p. 33-68.

2. Saller, H. A. and Rough, F. A., The Alloys of Uranium, Proceedings of the International Conference on the Peaceful Uses of Atomic Energy, Vol. 9, paper P/558, p. 107-116.

3. Pfeil, P. C. L., Alloys of Uranium and Thorium, Proceedings of the International Conference on the Peaceful Uses of Atomic Energy, Vol. 9, paper P/416, p. 117-119.

4. Cabane, G., Englander, M., Lehmann, J., Low Aluminum Uranium-Aluminum Alloys, Proceedings of the International Conference on the Peaceful Uses of Atomic Energy, Vol. 9, paper P/352, p. 120-137.

5. Saller, H. A., Preparation, Properties and Cladding of Aluminum-Uranium Alloys, Proceedings of the International Conference on the Peaceful Uses of Atomic Energy, Vol. 9, P/562, p. 214-220.

6. Fisher, E. S., Preparation of Alpha Uranium Single Crystals by a Grain Coarsening Method, Trans. AIME, 209:882 (1957).

7. Berlincourt, T. G., Reports NAA-SR-1885 and NAA-SR-1713 of North American Aviation. Edited by J. H. Hove and C. E. Dixon (1956).

8. Hein, R. A., Henry, W. E., and Wolcott, N. M., Superconductivity of Uranium, Physical Review, 107:1517 (1957).

9. Bridge, J. R., Schwartz, C. M., and Vaughan, D. A., X-ray Diffraction Determination of the Coefficients of Expansion of Alpha Uranium, Trans. AIME, 206:1282 (1956).

10. Lloyd, L. T., Discussion to Reference (9); Trans. AIME, 209:532 (1957).

11. Schuch, A. F. and Lacquer, H. L., Low Temperature Thermal Expansion of Uranium, Physical Review, 86:803, (1952).

12. Unpublished Information, Metallurgy Division - ANL.

13. Klepfer, H. H. and Chiotti, P., Characteristics of the Solid State Transformations in Uranium, Report No. ISC-893, Iowa State College, June, 1957.

14. Fisher, E. S. and McSkimin, H. J., The Adiabatic Elastic Moduli of Single Crystals of Alpha Uranium, submitted for publication.

15. Hearmon, R. F. S., The Elastic Constants of Anisotropic Material - II, Advances in Physics, 5:323 (1956).

16. Rothman, S. J., The Mechanical Properties of Uranium - A Monograph. In preparation for publication at ANL.

17. Lloyd, L. T. and Chiswik, H. H., Deformation Mechanisms of Alpha Uranium Single Crystals, Trans. AIME, 203:1206-1214 (1955).

18. Chiswik, H. H. and Kelman, L. R., Thermal Cycling Effects in Uranium, Proceedings of the International Conference on the Peaceful Uses of Atomic Energy, Vol. 9, P/557:147-158.

19. Powell, G. W., Klein, J. L., and Krashes, D., Private Communication. Nuclear Metals, Inc.

20. Gardner, H. R. and Riches, J. W., The Effect of Transformation Cooling Rate on the Activation Energy Required for Recrystallization of Beta Quenched Uranium, Preprint #17. Nuclear Engineering and Science Conference, March 17-21, 1958.

21. McDonell, W. R., Kinetics of the Beta Transformation of Uranium, Preprint #172, Nuclear Engineering and Science Conference, March 17-21, 1958.

22. Zegler, S. T. and Chiswik, H. H., Effects of Alloying Element Additions of Mo, Si, Al, Ti, V, and Nb on the Thermal Cycling Stability of Uranium, Paper No. 57-NESC-14, Nuclear Engineering and Science Conference, March 11-14, 1957.

23. White, D. W., Transformation Kinetics in Uranium-Chromium Alloys, Trans. AIME, 203:1221-1228 (1955).

24. Hayward, B. R. and Rowley, G. L., Dimensional Changes Resulting from Alpha-Beta Thermal Cycling of Uranium and Uranium Alloys, Report NAA-SR-1434, North American Aviation, Inc. (1956).

25. Saller, H. A. and Rough, F. A., Compilation of U.S. and U. K. Uranium and Thorium Constitutional Diagrams, Report No. BMI-1000, Office of Technical Services, Department of Commerce, Washington, D. C. (1955).

26. Summers-Smith, D., The Constitution of Uranium-Zirconium Alloys, Journal of the Inst. of Metals, 83:277 (1955).

27. Duffey, J. F. and Bruch, C. A., Delta Phase Field of the U-Zr Equilibrium Diagram, Transactions Metallurgical Society, AIME, 212, No. 1: 17-19, (1958).

28. Boyko, E. K., The Structure of the Delta Phase in the U-Zr System, Acta Crystallographica, 10:712 (1957).

29. Mueller, M. H., Knott, H. W., and Heaton, L. R., The Hexagonal Phase Found in Certain Zirconium and Titanium Alloys, Abstract of Paper presented at Pittsburgh Diffraction Conference, Nov. 6-8, (1957).

30. Silcock, J. M., Intermediate Phase in the Uranium-Zirconium System, Transactions AIME, 9:521 (1957).

31. Saller, H. A., Rough, F. A., and Bauer, A. A., The Effect of Oxygen on Zirconium-Uranium Epsilon (Delta) Phase Alloys. Paper No. 57-NESC-20, Nuclear Engineering and Science Conference (1957).

32. Kittel, J. H., Paine, S. H., and Chiswik, H. H., Influence of Heat Treatment on Irradiation-Induced Dimensional Changes in Some U-Zr Alloys, Symposium on Radiation Effects on Materials, ASTM Special Technical Publication No. 208:87-99 (1956).

33. Rogers, B. A., Atkins, D. F., Manthos, E. J., and Kirkpatrick, M. E., Uranium-Niobium Alloy Diagram, Paper 57-NESC-5, Nuclear Engineering and Science Conference (1957).

34. Dwight, A. E. and Mueller, M. H., Constitution of the Uranium-Rich U-Nb and U-Nb-Zr Systems, Report ANL-5581 (1957).

35. Draley, J. E., Greenberg, S., and Ruther, W. E., The High Temperature Aqueous Corrosion of Uranium Alloys Containing Minor Amounts of Niobium and Zirconium. Report ANL-5530 (1957).

36. Foote, F. G., Use of Plutonium in Nuclear Reactors. Information Conference of Nuclear Energy for Management, Sponsored by Organization for European Economic Cooperation, Amsterdam, June 24-28, 1957.

37. Kelman, L. R., Fast Reactor Fuel Development at Argonne National Laboratory. Paris Conference on Fuel Element Technology, Nov. 18-22, 1957.

38. Schonfeld, F. W., Phase Diagrams Studied at Los Alamos, Conference on Metal Plutonium, Sponsored by AEC and ASM, Chicago, Nov. 4-5, 1957.

39. Coffinberry, A. S. and Ellinger, F. H., The Intermetallic Compounds of Plutonium, Proceedings of the International Conference on the Peaceful Uses of Atomic Energy, Vol. 9:140 (1956).

40. Feder, H. M., Pyrometallurgical Processing of Nuclear Fuels, Proceedings of International Conference on Peaceful Uses of Atomic Energy, Vol. 9:586, (1955).

41. Schraidt, J. H., Pyrometallurgical Processing: Economics and Proposed Engineering Application, TID-7534. Symposiums on the Processing of Irradiated Fuels, Brussels Conference, 667-718 (1957).

42. Koch, L. J., Fast Breeder Power Reactors, Nucleonics, 68, March 1958.

43. Park, J. J., Private Communication. National Bureau of Standards.

44. Heal, T. J. and Williams, G. I., Compounds of Uranium with the Transition Metals of the Second and Third Long Periods, Acta Cryst., 8:494, (1955).

45. Saller, H. A., Dickerson, R. F., Bauer, A. A. and Daniel, N. E., Properties of a Fissium-Type Alloy, Report No. BMI-1123, Battelle Memorial Institute, August 1956.

46. Koch, L. J., Engineering Report on EBR-II, Report No. ANL-5788 in preparation for publication.

47. Unpublished Information, Reactor Engineering Division, ANL.



☆ U. S. GOVERNMENT PRINTING OFFICE : 1958 O— 468968 (J-1338)